MALEIC ANHYDRIDE COMPATIBILIZED PEACH WASTE AS FILLER IN POLYPROPYLENE AND HIGH DENSITY POLYETHYLENE BIOCOMPOSITES

A Thesis

presented to

the Faculty of California Polytechnic State University,

San Luis Obispo

In Partial Fulfillment

of the Requirements for the Degree

Master of Science in Food Science

by

Caralyn Bibi Araya Wong

August 2020

COMMITTEE MEMBERSHIP

TITLE:	Maleic anhydride compatibilized peach waste as filler in polypropylene and high density polyethylene biocomposites
AUTHOR:	Caralyn Bibi Araya Wong
DATE SUBMITTED:	August 2020
COMMITTEE CO-CHAIR:	Stephanie Jung, Ph.D. Department Head, Food Science and Nutrition Department
COMMITTEE CO-CHAIR:	Joongmin Shin, Ph.D. Associate Professor, Industrial Technology and Packaging Department
COMMITTEE MEMBER:	Ajay Kathuria, Ph.D. Associate Professor, Industrial Technology and Packaging Department
COMMITTEE MEMBER:	Luis Fernando Castro, Ph.D. Associate Professor, Food Science and Nutrition Department

ABSTRACT

Maleic anhydride compatibilized peach waste as filler in polypropylene and high density polyethylene biocomposites

Caralyn Bibi Araya Wong

It is estimated that roughly 103, 515 tons of peach waste is produced annually in the US. The majority of the waste is disposed of in landfills, which contributes to climate change as they release 93 million metric tons of CO_2 equivalent. Peach waste principally consists of remaining stone and seed after flesh removal. The agro-waste includes both cellulose and lignin, which can be utilized as a filler in plastic packaging to reduce carbon footprints and material cost. The objectives of this research are (1) to develop peach flour (PF)-filled biocomposites with a polyolefin matrix using maleic anhydride-g-high density polyethylene (MAH-g-HDPE) coupling agent resin and (2) to investigate the composites' physicomechanical, thermal, and water absorbance changes. First, preliminary experiments examined a range of PF concentrations (5-50%) and MAH concentrations (0-17%) were tested to narrow the variability of PF and MAH loading mixture in an HDPE matrix. Preliminary experiments suggested that a 2:1 ratio of PF:CR provides maximum tensile properties.

Response surface methodology (RSM) was utilized to analyze and optimize the tensile strength of the PW composite. The RSM parameters were MAH loading (5-20%), PF loading (2.5-10%), and polyolefin matrix (HDPE or polypropylene). The properties of PF-HDPE biocomposites were analyzed using several instrumental analyses. Mechanical strength (including tensile strength, elongation, and Young's modulus) and thermal

properties (thermal degradation, melting point, and crystallinity), and water resistance with the addition of PF and MAH were investigated.

Biocomposite mechanical properties generally resulted in a nonsignificant decrease compared to the controls. Water absorption significantly increased with PF loading ($P<0.01$, $\alpha=0.05$). PF-PP biocomposites demonstrated a shift in thermal stability with an average 9.6% increase in T_d compared to its control, whereas PF-HDPE biocomposites displayed no change in T_d compared to its control. PF-PP and PF-HDPE biocomposites experienced a 36.7% and 16.0% decrease, respectively, in crystallinity with PF addition. The results provided evidence that peach byproduct can be diverted from landfills and utilized a filler in a polyolefin matrix. Polyolefin biocomposites with 2.5% PF would possess comparable tensile strength to a commercially available control. PF-polyolefin biocomposites can be used for packaging, automotive, and non-weightbearing construction parts.

Keywords: Biocomposite, Peach stone, Maleic anhydride

Acknowledgements

I would like to thank my advisors, Dr. Stephanie Jung and Dr. Joongmin Shin, for the opportunity to perform this research project as well as their guidance throughout my time in this program. I would also like to thank my committee members, Dr. Ajay Kathuria for his time and dedication in the lab, and Dr. Luis Castro for his feedback and always checking in on my progress. I want to thank Dr. Haotian Zhang from the Dairy Science Department and Dr. Mark Edwards for the Animal Science Department for both helping me perform proximate analysis on the peach flour samples.

The faculty and staff of the Food Science and Nutrition Department were always very supportive in both my research and academic journey throughout my career at Cal Poly. I'd like to thank Molly Lear for her time and advice and always being very flexible with scheduling time in the Pilot Plant. Much appreciation for Renata Lehman for helping with processing the peach stones into flour.

Finally, I'd like to thank my friends and family for their endless support and love throughout my undergraduate and graduate education.

The peach stones were generously donated by Del Monte, Inc. Thank you Doug Van Diepen from Del Monte, Inc. for his time and willingness to collaborate on this project.

TABLE OF CONTENTS

Page

List of Tables

Page

List of Figures

Page

List of Equations

Page

List of Most Commonly Used Abbreviations

PP = Polypropylene

HDPE = High-density Polyethylene

MAH = Maleic Anhydride

PF = Peach Flour

CR = Compatibilizer Resin

DOE = Design of Experiment

CCD = Central Composite Design

CHAPTER 1 – INTRODUCTION

1.1 Background information

Food is lost and wasted along the entire supply chain with the agricultural production and consumer consumption stages accounting for a majority of food wastage (Figure 1.1). Food loss refers to the unintended result of an agricultural process or technical limitation in storage, infrastructure, and/or packaging. Food waste refers to food that is safe for consumption but gets discarded. The fruit industry generates large volumes of waste and byproducts from processing fresh fruit into juices, nectars, jellies, and canned foods. Fruit byproducts such as peels, stems, and seeds account for more than 50% of fresh fruit weight and may have a higher nutritional or functional content than the final product (Ayala-Zavala et al. 2011; Torres-León et al. 2018).

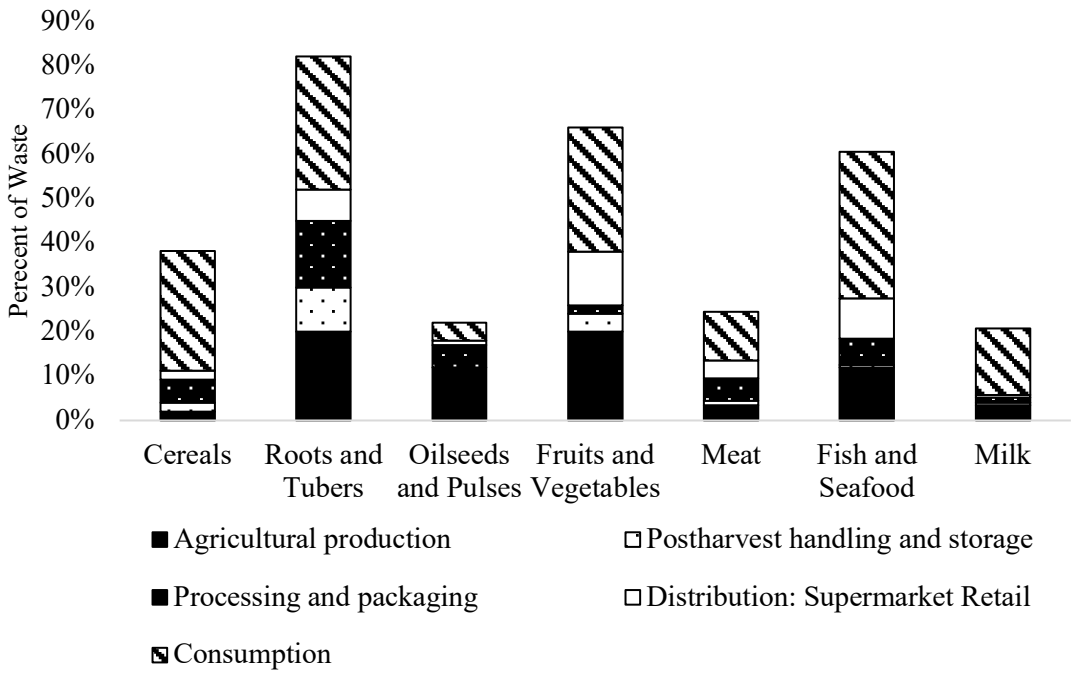

Figure 1.1: Estimated food waste percentages for each commodity group in each step of the food supply chain in North America and Oceania (Adapted from FAO 2011).

Landfilling remains the main option for managing food waste, but this method results in landfill gas and leachate production with the risk of contaminating ground

water (Kaur et al. 2019). Municipal solid waste landfills are the third-largest human-generated source of methane emissions in the United States, releasing 92.8 million metric tons of carbon dioxide equivalent in 2017 alone (EPA 2019). Methane is a potent greenhouse gas with a global warming potential 28 times that of carbon dioxide (IPCC 2013). Options such as anaerobic digestion and composting are more beneficial methods of organic waste management as they return our organic resources to the Earth as soil amendment. Therefore, enforcing waste management practices to divert organic waste from the landfill is a viable alternative to reduce methane emissions and mitigate global climate change.

In 2017, the United States peach industry produced 59,410 tons of by-product (15% total weight) after producing 396,070 tons of processed peach (Hills and Roberts 1982; USDA NASS 2020). Peaches may be processed for canning, freezing, or juicing. Processed peach waste includes peels, pulp, trimmings, stems, and stones. The majority of waste is in the form of peach stones, which are most commonly sent to landfill (Wu et al. 2018). Fruit byproduct are rich in proteins, fibers, and polyphenols, which have the potential for use in nutraceutical supplements, food additives, and pharmaceutical products to recover waste and reduce the environmental impact and enhance economic value (Ayala-Zavala et al. 2011).

The peach is an example of a drupe, a type of fruit in which an outer fleshy part surrounds a shell that contains the fruit seed. Other drupes include cherries, coffee berries, walnuts, and coconuts. Biochemical analysis of drupe shells indicates that they contain nearly twice as much lignin as wood and possess high mechanical properties, which opens opportunities for drupes in materials research (Mendu et al. 2011).

The soaring price for virgin plastic and the negative environmental impact of plastic waste has directed the plastic industry to search for a cheap, eco-friendly plastic substitute (Sherman 2019). This has led to the development of polymer matrices reinforced with natural fillers, such as flax, hemp, and jute (Gurunathan et al. 2015). This material is called a biocomposite. The natural fillers are generally sourced from agro-waste of food processing facilities to reduce the impact of the food production cycle. Plant and wood-based fibers possess relatively high strength, high stiffness, and low-density characteristics compared to their synthetic filler counterpart (Alemdar and Sain 2008). These are important properties as they have an important impact on mechanical performance and strength of biocomposites. However, the hydrophilicity of natural fibers limits their compatibility with hydrophobic polymer matrices. To improve their compatibility, natural fibers can be exposed to different treatments to improve interfacial adhesion between the two phases. Both physical and chemical treatments of natural fibers have been explored. Physical methods increase the mechanical bonding and entanglements between fiber and matrix to enhance interfacial adhesion, while chemical treatments may activate hydroxyl groups or introduce moieties that interlock with the polymer matrix (Herrera Franco and Valadez-González 2005; Ghasemi et al. 2018). Maleic anhydride addition has shown to be a great way to improve interaction. For example, the use of a maleic-anhydride-grafted-polypropylene (MAH-g-PP) coupling agent in a barley husk and coconut shell-polypropylene composite increased the tensile strength 20-30% due to ester linkage formation between the polypropylene (PP) matrix and fibers' cellulose molecules (Bledzki et al. 2010).

In this study, thermoplastics, high-density polyethylene (HDPE) and PP, are used to make the biocomposite. Thermoplastics are generally favored over thermosets because of their recyclability (Faruk et al. 2012). HDPE and PP are the most common thermoplastics for biocomposite applications, partly due to their low melting point at 200°C, which allows for processing without the thermal degradation of natural fibers (Pickering et al. 2016). PP is widely used for industrial and household composite items due to its low production cost, design flexibility, and suitability for filling and blending (Amir et al. 2017; Dinh Vu et al. 2018). HDPE is one of the dominant rigid plastics in the packaging industry as it meets the performance, aesthetic, and economic needs of rigid packaging (Cornell 2007). Primary rigid plastic applications include bottling water, milk, food, and household chemicals.

1.2 Approaches

Processed peach waste in the form of peach stones were incorporated into a polyolefin matrix using a maleic anhydride coupling agent. The peach stones were milled into peach flour (PF) (Particle size ~180 μm) via a grain mill. Preliminary experiments and a design of experiment (DOE) was executed to understand the effect of peach flour loading and coupling agent concentration.

The objectives of this research were (1) to develop PF-filled composites with a PP and HDPE matrix using MAH as a coupling agent resulting in a biocomposite with maximum tensile strength and (2) to investigate the composites' physico-mechanical, thermal, and water resistance properties.

1.3 Research potential

A successful PF-polyolefin biocomposite has the potential to reduce organic waste sent to landfill, which will reduce landfill gas production. As the third highest peach producing country, an alternative peach waste management system has the potential to reduce the United States' overall methane production. A PF-polyolefin biocomposite may be a prospective material for manufacturing household items, automotive parts, and construction materials. Biocomposites are generally great options for car doors, chairs, dust trays, and nonstructural construction parts.

1.4 Statement of hypothesis

It was hypothesized that MAH compatibilized-PF would serve as a viable filler in a polyolefin matrix because peach stones offer a high lignin content for interaction between the compatibilizer and polymer matrix.

CHAPTER 2 – LITERATURE REVIEW

2.1 Peach production and processing

Peach, *Prunus persica* (L.) Batsch, originated from Northern China and dated back to Neolithic times. The Neolithic village, Yujao City, was discovered in 1973 and its excavations uncovered wild peach stones dating back to 6000-7000 BC (Chen, 1994). Peaches were introduced to the Americas through Spanish explorations in the 16th century. Currently, the top five countries in peach production are China (46%), Italy (9%), Spain (7%), USA (7%), and Greece (4%) (Bassi et al. 2015). There are almost 1.5 million hectares of peach orchards worldwide (Gradziel and McCaa 2008). In 2018 the United States consumption of fresh peaches per capita was approximately 2.2lbs, while apple consumption was 16.91lbs (Shahbandeh 2019). Peach varieties are categorized by the relationship of the fruits' flesh with their pit. Freestone peaches have pits that easily detach from the flesh, while clingstone peaches have flesh that clings to the pit. Freestone peaches are produced for the fresh market and clingstone peaches are produced for canned peaches. More than 90% of peach production is dedicated to the fresh market.

Peaches grow best in regions of temperate climates, between 30° and 40° latitude. A standard peach tree can grow to 25 feet tall and 25 feet wide if not pruned. Peaches prefer well-drained, sandy soil at a pH range of 6.0-6.5. Prior to harvest, peaches have a chill requirement of 600-900 hours at a temperature below 45°F. Peaches are usually harvested between late June and September. Peaches are usually harvested at 70-80% ripeness to be of optimum ripeness once it reaches the grocery store or cannery.

Peach processing begins with picking and collecting peaches in large bins. For prolonged storage, peaches are held in cold storage at 0-1°C and 85-90% relative

humidity. Controlled atmosphere storage is set at 0-1°C, 5% CO_2., and 1-3% O_2 (Gradziel and McCaa 2008). Fresh market peaches are brushed and washed twice to remove excessive peach fuzz. The peaches are sprayed with a coat of food grade wax to increase shelf-life and improve its appearance. Fresh peaches are sorted and graded based on their size and packed for distribution. On the other hand, processed peach products take washed and sorted peaches to a conveyor to be cut into halves. Vibrating conveyors are used to releasing the pit from the flesh. The removed stones fall through holes of the conveyor surface for collection. Peach halves are manually inspected to remove any remaining stones or pit fragments. The peach skin is removed with an 80°C lye solution. The fruit is then washed and inspected for blemishes. Blemished fruit is separated and used for purees and frozen fruit blends. The peach halves of acceptable color, taste, and texture are sorted by size again. The peach halves are then canned with a sugar solution. The canned peaches are passed through boiling water to cook the peaches and sterilize the cans. The cans are finally labeled and palletized for distribution.

2.2 Peach stone composition

Over time plants have evolved to adapt to their environment with intentions to survive and reproduce. Peaches have managed to protect their seeds with the use of the endocarp (Figure 2.1). Fruits with hardened endocarps are categorized as drupes. Drupes include mangoes, olives, plums, coconut, and coffee. The endocarp encases the fruit's seed and serves as a physical barrier to protect the seed from disease and herbivory.

Peach fruit growth is traditionally divided into four stages (Gradziel and McCaa 2008). The first stage is roughly a 50-day growth period between flower bloom and endocarp hardening. The exact length of the first stage is dependent on cultivar and

temperature. The second stage experiences little increase in fruit size, and energy is directed more towards endocarp development. The third stage is a period of rapid fruit size increase as mesocarp cells expand. The fourth stage is during the last few weeks before harvest and is a period of rapid sugar accumulation.

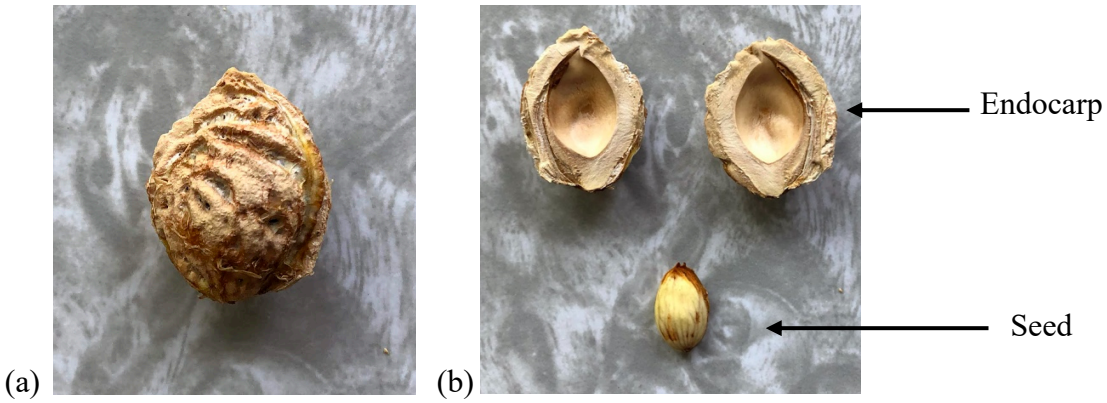

Figure 2.1: (a) A whole peach stone and (b) a deconstructed peach stone

Due to the structural similarities between peach endocarp tissue and wood, the secondary wall formation process can be inferred from wood formation (Dardick and Callahan 2014). Wood formation consists of five major developmental steps: (1) cell division, (2) cell expansion, (3) secondary cell wall deposition, (4) programmed cell death, and (5) heartwood formation (Déjardin et al. 2010). The primary cell wall provides the strength and flexibility needed for cell growth and is comprised of cellulose, hemicellulose, and pectin, whereas the rigid secondary cell wall primarily provides structure and is comprised of cellulose, hemicellulose, lignin, and smaller amounts for pectin and protein. Endocarp hardening occurs during secondary wall formation and lignification (Dardick and Callahan 2014).

Drupes, although classified by their similar anatomy, all contain unique tissue compositions (Table 2.1). The composition of plant tissue varies with species and growing conditions. The biochemical analysis of drupes including olive, black walnut,

peach, and coconut indicate that they contain nearly twice as much lignin as wood, suggesting that secondary wall formation is relatively extreme in fruit endocarp tissues (Mendu et al. 2011).

Table 2.1: Non-starch polysaccharide contents of various plant tissues

Fiber	Lignin (wt.%)	Cellulose (wt.%)
Apricot Stone[a]	37.0	30.0
Barley Husk[b]	22.0	39.0
Coconut Shell[c]	44.0	29.7
Olive Stone[c]	39.0	33.7
Peach Stone[c]	41.6	25.6
Soft Wood[b]	31.0	42.0
Walnut Shell[c]	40.4	28.2

[a]Rolando and Bjornbom 1999; [b]Bledzki et al. 2010; [c]Mendu et al. 2011

Cellulose is a linear, semicrystalline polysaccharide consisting of β −(1-4) linked D-anhydroglucopyranose units (Figure 2.2). Cellulose chains are bonded by van der Waals forces and hydrogen bonds in the microfibrils. Bundles of microfibrils are combined to form the cellulose fiber. Degree of polymerization of cellulose is between 1510 and 5500, which strengthens its crystallinity. Cellulose is reactive due to the hydroxyl groups on the glucose ring which can result in extensive hydrogen bonding.

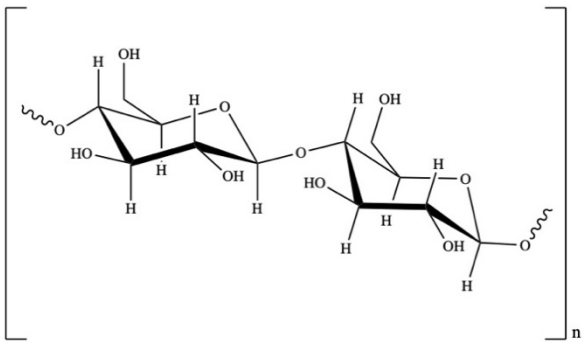

Figure 2.2: Cellulose structure

Hemicellulose is an amorphous and heterogeneously branched polymer of pentoses and hexoses, mainly D-galactose, D-xylose, D-mannose, L-arabinose, D-

glucose. Hemicellulose has a lower molecular weight compared to cellulose. Hemicellulose has a degree of polymerization between 50 and 200, which makes it amorphous and easily hydrolysable (Yang et al. 2019). Hemicellulose forms a supportive matrix for cellulose microfibrils (John and Anandjiwala 2008).

Lignin serves as a matrix for the cellulose and hemicellulose and contributes to the mechanical strength of the cell tissue. Lignin is formed via the phenylpropanoid pathway. This process produces lignin monomers, ρ-coumaryl, coniferyl, and sinapyl alcohols, which serve as the basis for lignification to produce the lignin polymer via oxidative reactions aided by peroxidases and laccases (Figure 2.3). The lignin monomers proceed with random coupling to a growing lignin chain to produce the complex lignin polymer. The phenylpropanoid pathway produces other secondary metabolic compounds that provide other fruit functions such as limiting bacterial and fungal disease and contributing to fruit flavor and aroma to both attract and deter herbivores (Dixon and Paiva 1995; Peters and Constabel 2002).

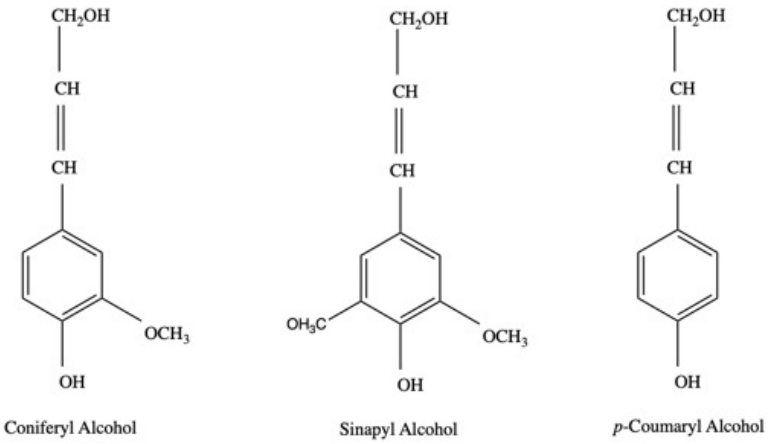

Figure 2.3: Lignin monomers

The peach endocarp encases an almond-like seed, rich in protein and oil. The peach seed has 23-27% and 17-21% of fat and protein, respectively (Pelentir et al. 2011).

The fatty acid composition is primarily oleic and linoleic acid (around 50% each), which is uncommon for vegetable oils (Annisa and Widayat 2018). The peach seed protein is rich in lysine, leucine, isoleucine, valine, threonine, basic and acidic amino acids with contents comparable to soybeans (Rahma and El-Aal 1988).

The seeds of different fruits such as peaches, plums, and apricots, contain a considerable amount of amygdalin, a toxic substance for human consumption (Table 2.2). Amygdalin contains a nitrile group, which can be released as toxic cyanide by the action of beta-glucosidase and cause cyanide poisoning. However, peaches have shown to have very low or undetectable levels of amygdalin in the endocarp and oil, which may have positive implications for its use in the food industry (Viorica-Mirela et al. 2006; Lee et al. 2017).

Table 2.2: Amygdalin content of stone fruit kernels (Excerpted from Bolarinwa et al. 2014).

Fruit	Amygdalin content (mg/g)
Apple	2.96±0.02
Apricot	14.37±0.28
Black Plum	10.00±0.14
Peach	6.81±0.02
Pear	1.29±0.04
Red Cherry	3.89±0.31

2.3 Fruit industry byproduct

The Food and Agriculture Organization (FAO) of the United Nations defines food waste as follows: “the decrease in quantity or quality of food.” Food waste is part of food loss and refers to discarding or alternative (nonfood) use of food that is safe and nutritious for human consumption along the entire food supply chain, from primary production to end household consumer level.

Food loss and waste can occur for several reasons at every stage of the production and supply chain. Food loss refers to the decrease in quality or quantity of food lost in the supply chain due to agricultural processes and/or technical limitations, whereas food waste refers to the discarding of food that is safe and nutritious for human consumption (FAO 2019). Americans waste 30-40% of the U.S. food supply, representing a loss of energy and resources spent to produce, process, and transport food. This excessive food waste also contradicts the growing demand for food as population increases (Ehrlich and Harte 2015). In October 2018, the U.S. Department of Agriculture (USDA), the U.S. Environmental Protection Agency (EPA), and the U.S. Food and Drug Administration (FDA) signed a formal agreement under the *Winning on Reducing Food Waste Initiative* to align efforts to reduce food waste and loss in the United States (Formal Agreement Relative to Cooperation and Coordination on Food Loss and Waste, 2018). This combined effort will include better education and outreach programs, volunteer programs, public-private partnerships, research, and policy discussion.

The United Nations Food and Agriculture Organization (FAO) has estimated that losses and waste in fruits and vegetables may reach 60%, being among the highest among all types of foods. As the consumer demand for more fresh, ready-to-eat foods increases, the amount of food waste from the fruit and vegetable industry continues to grow. The waste is composed of seed, skin, rind, and pomace, which can be used for a number of value added products with applications in food, pharmaceutical, and allied industries (Wadhwa et al. 2016; Sagar et al. 2018). Despite the high value of such waste, Americans had landfilled or incinerated over 50 million tons of compostable waste in 2015 alone (Bradford et al. 2019).

Landfilling remains the main technology for managing food waste, but this method results in landfill gas and leachate production with the risk of contaminating groundwater (Kaur et al. 2019). Landfill gas is generated from the disposal of biodegradable materials in landfills and is composed of 55-65% v/v methane and 40-45% v/v carbon dioxide (Aghdam et al. 2019). Municipal solid waste landfills are the third-largest human-generated source of methane emissions in the United States, releasing 95.6 million metric tons of carbon dioxide equivalent in 2018 alone (EPA 2020a). Methane is a potent greenhouse gas with a global warming potential 28 times that of carbon dioxide (Dentener et al. 2013). The gas collection efficiency of landfills range from 36-85% with an average of 75% (Barlaz et al. 2009; EPA 2011). Methane, however, is a valuable resource used to power many homes and is required to be collected by the Clean Air Act, but only 21.5% landfills are held under this requirement (EPA 2020b). Only landfills with capacities greater than 2.5 million cubic meters are required to install a gas collection system and the average American landfill is only 600 acres or 740k cubic meters. This leaves over 2,000 landfills to continue to release landfill gasses into the atmosphere. Therefore, enforcing waste management practices to divert organic waste from the landfill is a viable alternative to reduce methane emissions and mitigate global climate change.

2.4 Peach waste valorization

Peach processing generates waste as peels, seeds, trimmings, and water. The main disposal methods for peach processing are landfill (63%), liquid waste (5%), animal feed (17%), and other by product (15%) (Katsuyama et al. 1973, Wu et al. 2018). The peach stone is roughly 18% of the total fruit weight (Kaynak et al. 2005). Peach stones are

considered to be an agricultural waste in orchards and are most commonly sent to landfill (Wu et al. 2018). Currently, peach seed products in the market include cosmetic peach seed oil and peach seed dietary supplements. Peach seeds have been used in Chinese medicine to treat inflammation and allergies. In terms of industrial uses, Del Monte's canning facility in Greece burns peach pits to generate steam which saves nearly 587,000 kg of fuel oil annually (Del Monte 2014).

The upcycling of peach waste has been explored for applications in hydrogen production, water purification, and boiler fuel (Rabaçal et al. 2013; Marković et al. 2015; Argun and Dao 2017). The feasibility of stone fruit use in materials development has been explored in various drupes including apricot and peach. For example, the apricot shell was added to an HDPE biocomposite while blended peach and apricot shell wastes were used for a bio-based concrete (Essabir et al. 2014; Wu et al. 2018). Despite a few studies available, the use of peach and apricot shells for materials production is limited and leaves room for opportunity.

2.5 Biocomposites

A growing trend in the plastic industry is the use of natural fibers as reinforcement in polymer matrices to create materials termed biocomposites. Natural fibers used in composites are typically sourced from plants and animals. Plant fibers are categorized into subdivisions by their composition, such as starch-based, ligno-cellulosic, etc. (Figure 2.4) (Gurunathan *et al*. 2015). Biocomposites have been developed using extracted xylan from rapeseed straw in a poly(ε-caprolactone) (PCL) matrix, argan nut shell in a PP matrix, and sea grass (*Posidonia oceanica*) leaves in a poly(lactic acid) matrix (Svärd *et al*. 2018, Essabir *et al*. 2016, Scaffaro *et al*. 2011). The advantages of

natural fibers include low cost, biodegradability, renewability, and high availability (Calabia et al. 2013). The performance enhancements of biocomposites include specific mechanical properties and lower density, compared to the conventional glass fiber reinforced composites (Beigbeder et al. 2019). Silk fiber-poly(butylene succinate) (PBS) biocomposite material demonstrated a tensile strength and modulus improvement of 27% and 160%, respectively, compared to the unreinforced PBS control (Han et al. 2006). Biocomposite materials have applications in aerospace, automotive, construction, and packaging industries. The low density of biocomposites is ideal for automotive and aerospace applications because it would minimize vehicle mass, leading to lower vehicle inertia forces and less fuel burned to carry the car mass, which would have an overall result of reducing CO_2 emissions (Fan et al. 2011).

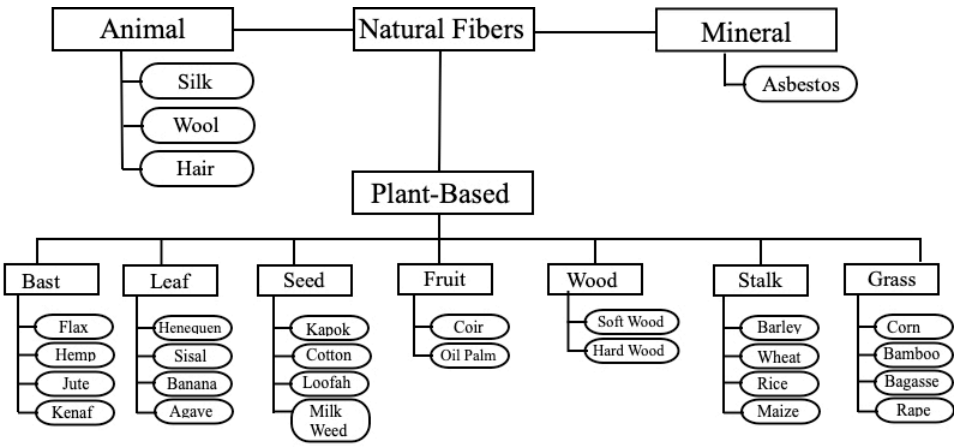

Figure 2.4: Diagram representing the various sources of natural fibers (Adapted from Gurunathan et al. 2015).

Natural fibers are composed of cellulose, hemicellulose, lignin, pectin, waxes, and water soluble substances. Cellulose contains a large amount of hydroxyl groups capable of forming hydrogen bonds for crystalline packing to benefit mechanical properties of composites, but hydroxyl groups also impart poor interface and poor resistance to moisture absorption due to their hydrophilicity (Onuaguluchi and Banthia 2016).

Hemicellulose persists of an open structure with hydroxyl and acetyl groups, which makes them hydrophilic, soluble in alkali, and easily hydrolyzed in acids (John and Anandjiwala 2008). Lignin reduces water uptake, improves thermal stability, and improves fiber matrix adhesion within biopolymers (Graupner 2008; John and Anandjiwala 2008).

The primary drawback of biocomposites is the poor compatibility between the hydrophilic natural fibers with hydrophobic polymer matrices, which leads to undesirable performance properties (Calabia et al. 2013). Poor composite strength results from the lack of stress transfer from the polymer matrix to the natural fibers (Rana et al. 1998; Yang et al. 2019). However, physical and chemical fiber treatments can be used to improve undesirable properties by improving the adhesion of natural fibers with polymer matrices.

2.5.1 Fiber treatment

2.5.1.1 Chemical treatments

Chemical modifications aim to modify the fiber surface and increase fiber strength (Li et al. 2007). Alkali treatment or mercerization is one of the most common treatments for natural fibers. Sodium hydroxide (NaOH) is used to disrupt hydrogen bonds of the cellulose network to increase surface roughness, promote ionization, and remove some lignin, wax, and oil on the fiber surface (Li et al. 2007, 2009). The mercerization treatment submerges fibers in NaOH solution at specified conditions (concentration, temperature, time, pressure), which will depend on the lignin and its source. Previous treatment conditions used include 2% alkali solution for 90 seconds at 200°C and 5% alkali solution for up to 2-72 hours at room temperature to treat sisal and

hemp fibers, respectively (Garcia-Jaldon et al. 1998; Mishra et al. 2001). Alkaline treatment has two major effects: (1) increasing surface roughness for enhanced mechanical interlocking and (2) increasing cellulose exposure to increase the number of reaction sites. Alkaline treatment has been found to give a 30% increase in tensile properties (Valadez-Gonzalez et al. 1999; Van de Weyenberg et al. 2003).

Acetylation is an esterification reaction that introduces an acetyl group (CH_3COO^-) to an organic compound (cellulose fibers) and causes plasticization. The reaction substitutes hydroxyl groups of the cellulose fibers with acetyl groups to modify polymer properties so they become hydrophobic (Hill et al. 1998). Acetylation can also increase surface roughness for better interlocking to increase dimensional and thermal stability (Li et al. 2007). The acetylation process involves alkaline treatment followed by acetylation. Raw sisal fibers were treated in 18% NaOH solution, glacial acetic acid solution, and finally acetic anhydride with one drop of concentrated H_2SO_4 for 1 hour and resulted in enhanced adhesion with a polystyrene matrix and higher thermal stability (Manikandan Nair et al. 2001).

Coupling agents are described as a class of adhesives used to bond polymers with fibers and fillers (DeArmitt and Rothon 2017). Coupling agents modify both the fiber surface and polymer matrix to enhance interfacial bonding and improve mechanical properties in composites (Gassan and Bledzki 1997). The bonded interfaces may also reduce water absorption giving improved property retention and electrical stability under wet conditions (DeArmitt and Rothon 2017).

MAH is one of the most popular and most efficient coupling agents for starch-containing composites with both biodegradable and non-biodegradable polymer matrices

(Jiang and Zhang 2017). The success of MAH in industry is attributed to MAH's ability (1) to be readily grafted onto polyolefins, (2) to be economically produced, and (3) to impart relatively high performing mechanical properties (Keener et al. 2004). Coupling agents composed of grafted MAH can increase mechanical properties up to 40% with an optimized coupling agent-fiber surface ratio (Endres et al. 2006).

The grafting reaction can be carried out in solution or in the molten state, however the low cost and process feasibility of melt mixing deems it as the preferred method (Rzayev 2011). The process of grafting MAH onto a polyolefin involves a reaction between the polymer melt with MAH in the presence of organic peroxides (Figure 2.5). The peroxides' weak O-O bonds break to produce free radicals in the form of RO* (the asterisk represents an unpaired electron). The radical attracts hydrogen atoms from the polyolefin chain forming a macroradical initiating the grafting process. Following, MAH monomers bond to the macroradical to form the functionalized polyolefin. The occurrence of a β-scission reaction is argued to take place after functionalization. Studies have found evidence of extensive β-scission after MAH grafts on to tertiary carbons as it causes a decrease in molecular weight with increasing MAH initial concentration (Zhang et al. 2005).

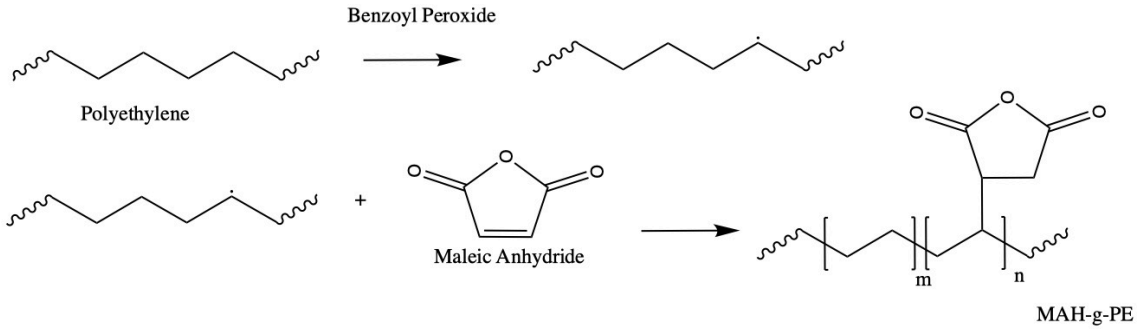

Figure 2.5: Scheme diagram of PE grafted with MAH (Adapted from Zhang et al. 2017).

Optimizing the grafting process involves several variables such as type and concentration of peroxide and MAH, reaction time and temperature, rotor speed, addition sequence of reagents, and the presence or lack of stabilizers. Peroxides of low volatility and good solubility with the polyolefin melt are selected to promote macroradical production and prevent radical decomposition (Passaglia et al. 2009). Melt reactions typically occur in a mixer at 180-240°C. Co-rotating extruders have shown to be more successful than counter-rotating extruders because of the enhanced temperature control and mixing operation (Kim and White 1995). The chemical and physical properties of coupling agent-grafted-polymers vary with manufacturer and resin application (Table 2.3).

Table 2.3: Coupling agent properties (Excerpted from Correa et al. 2007)

Coupling Agent	**Material Code**	**Manufacturer**	**MAH (%)**	**M_n (g/mol)**	**M_w (g/mol)**	**Polydispersity M_n / M_w**
Orevac®	CA-100	Atofina	1.0	8822	94328	10.7
Polybond ®	PB-3200	Crompton	2.5	12308	97456	7.9
Epolene®	E-43	Eastman	3.7	1775	20171	11.4
Epolene®	G-3003	Eastman	0.8	8031	84400	10.5

The coupling mechanism between natural fiber and maleic anhydride is not clearly understood yet, however previous research has hypothesized potential bonding mechanisms (Figure 2.6). Literature suggests that an esterification reaction and H-bond

interactions may take place at the interface of the natural fiber and compatibilized polymer.

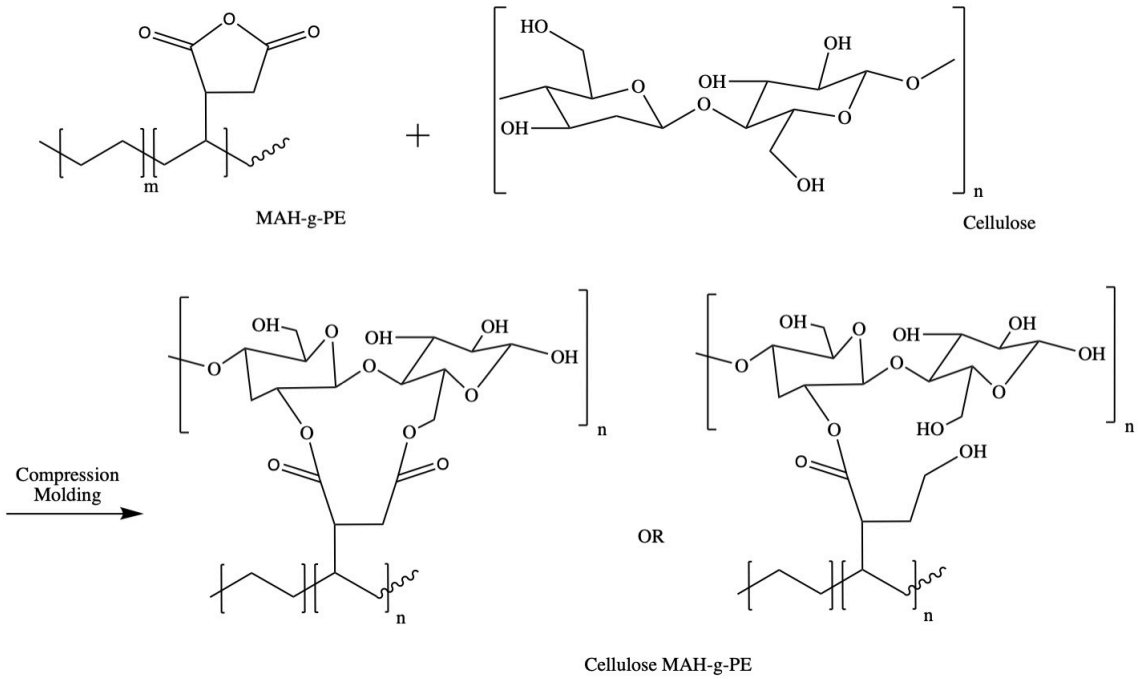

Figure 2.6: Potential mechanism bonding interactions between cellulose and MAH-g-PE (Adapted from Correa et al. 2007; Hermawan et al. 2017).

2.5.1.2 Physical treatments

Physical treatments, such as plasma and heat treatment, aim to (1) remove surface contamination and create a low energy-interface between dissimilar materials and (2) roughen the fiber surface to enhance the contact area and facilitate mechanical interlocking (Mukhopadhyay and Fangueiro 2009; Venkatachalam et al. 2016). The simplest physical treatment is a heat treatment with optimized temperature, time, and atmosphere conditions to reduce fiber moisture content and increase cellulose crystallinity to improve tensile and flexural strength (Rong et al. 2001). Plasma treatment bombards a substrate with electrical currents and magnetic fields causing electrons to collide and chemical bonds to break on the material's surface, which ultimately results in surface chemistry and topography changes (Roy Choudhury 2017). Plasma treated jute

fibers exhibited higher hydrophobicity likely due to fiber oxidation or a decrease in phenolic and secondary alcohol groups and a 14% increase in flexural strength due to new bond formations (Sinha and Panigrahi 2009). Recent interests in eco-friendly fiber treatments have led to innovative methods using enzymes and fungi, which are found to be economical, require less energy, improve fiber thermal stability, and are selective towards pectin and hemicellulose removal (Pickering et al. 2007; George et al. 2014; Väisänen et al. 2018).

2.5.2 Fiber characteristics

Fillers are materials added to resins to improve specific properties and decrease product cost. There are inherent differences in physical and chemical structures between fillers that influence their compatibility with polymer matrices (Table 2.4). For the application of biocomposites, fillers are bio-based and are sourced from a variety of plants, animals, or minerals. Many countries have banned the use of minerals due to associated health issues and animal fibers generally possess weaker strengths and stiffness compared to plant fibers, therefore plant fibers are the preferred choice of alternative filler (Pickering et al. 2016).

Fiber geometry is one of the most important factors of composite materials that influence mechanical properties. Industry prefers a particle size <300μm because it has been found to increase tensile modulus by creating strong interfacial bonding between the fiber, coupling agent, and polymer matrix (Nourbakhsh et al. 2010). Studies have established that there is a positive relationship between composite strength and fiber length, however the increase in strength remains unchanged after the fiber length has reached a certain level for both synthetic and bio-based fillers (Miwa and Horiba 1994;

Bledzki et al. 2015). A study of four different natural fiber composites resulted in composites with different mechanical properties likely due to varying fiber height to width ratios (called the aspect ratio), fiber thicknesses, and cellulose microfibril alignment (Bledzki et al. 2015). Higher aspect ratios positively affected composite strength and heat deflection temperature due to better matrix-fiber stress transfer and interface strength, respectively. Additionally, thicker fibers were found to absorb more impact energy, which increased fracture toughness (Fu and Lauke 1997). For example, a metal matrix determined that a braided metal was able to absorb more energy than unidirectionally laminated metal because of the thickness reinforcement of the braided structure which limited matrix cracks and bends (Lee 1993).

Table 2.4: Dimensions of common fibers (Excerpted from Rowell et al. 1997).

Fiber	**Average Length** (mm)	**Width** (mm)
Cotton	10-60	0.02
Flax	5-60	0.012-0.027
Hemp	5-55	0.025-0.050
Bamboo	1.5-4	0.025-0.040
Cereal Straw	1-3.4	0.023
Jute	1.5-5	0.02
Deciduous Wood	1-1.8	0.03
Coniferous Wood	3.5-5	0.025

The critical fiber length (L_c) is the minimum length at which fibers can carry their maximum load (Eq. 2.1). This critical length is dependent on the fiber strength (σ_f^*) and diameter (d) and on the fiber–matrix bond strength (τ_c) (Callister 2006). Fibers must be greater than their critical fiber length to impart a significant improvement of a composite.

$$L_c = \frac{\sigma_f^* d}{2\tau_c} \quad (2.1)$$

Fibers have lower decomposition temperatures than polyolefins, but still generally impart enhanced thermal stability in composites. Hemicellulose and cellulose are the least thermally stable and decompose between 150-350°C and 275-350°C, respectively. Lignin decomposes between 250-500° (Yang et al. 2005). Lignin may increase thermal stability due to its hydroxyl groups which may improve the stability of aromatic structures of its complex phenylpropanoid unit (Ghozali et al. 2017). Additionally, lignin's structure contributes less flammability due to high char ability, which is the ability to partially burn or blacken the surface. Therefore, as lignin content increases, the amount of thermal residue increases.

2.5.3 Biocomposite matrices

Biocomposites can be constructed with petroleum-based or bio-based polymers. Biopolymers are plastics produced from petroleum-based or renewable biomass sources, and may be triggered biodegradable. Poly(lactic acid) (PLA) is identified as the most reliable bio-based alternative to conventional plastics and other biopolymers due to promising thermal and mechanical properties similar to PET and PP, respectively (Barletta et al. 2017). Cellulose fiber enforced PLA displayed significantly higher tensile strength and Young's modulus compared to PP-based composite likely because of the less hydrophobic character of PLA, which allows for better fiber-matrix adhesion (Graupner and Müssig 2017). However, PLA is considered expensive and its physical properties such as brittleness limits its applications only to specialty fields, such as

biomedical solutions in resorbable materials and surgical implants (Barletta et al. 2017; Dinh Vu et al. 2018).

Among the polyolefins, polypropylene (PP) and PE are the most produced and consumed (Gopanna et al. 2019). The industry favors synthetic polymers because of their highly desirable properties, such as strength, flexibility, and chemical resistance (Nagalakshmaiah et al. 2019). PP and PE are widely used to manufacture industrial and household items, especially as a matrix material in composites, due to their low cost, design flexibility, and recyclability (Drzal et al. 2001; Dinh Vu et al. 2018). Several advantages of PP include transparency, dimensional stability, and its suitability for filling, reinforcing, and blending (Amir et al. 2017). PE is extensively used for both nonstructural and structural applications and may be used for its toughness, low coefficient of friction, and low electrical conductivity (Mansor et al. 2018; Gopanna et al. 2019).

2.6 Biocomposite preparation

Biocomposites can be manufactured with the same technology as conventional plastic. Plastic manufacturing involves the conversion of solid plastic granules into a melt via extrusion. An extruder uses heat, shear, and pressure to melt the solid granules into a molten state for the next step of processing. The parts of an extruder include hopper, barrel, thermocouples, screw, and die (Figure 2.6). The hopper stores and feeds plastic granules as it travels into the barrel. The barrel, the main body of the extruder, is an externally heated hollow tube. The barrel typically has a temperature profile of increasing temperature zones monitored by thermocouples. The screw is the main working part of

the extruder housed inside the barrel. The helical channels of the screw melt and convey the plastic.

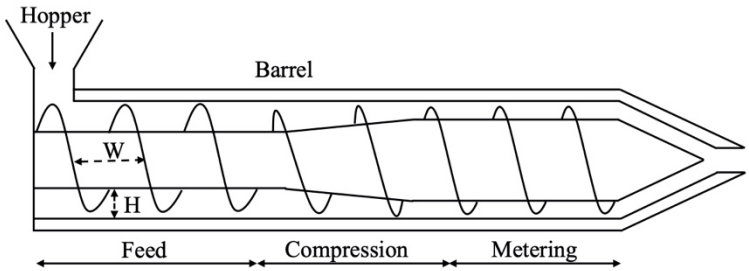

Figure 2.7: Schematic of a single-screw extruder (Adapted from Altınkaynak 2010).

The screw is divided into three sections: feed, compression, and meter. A standard screw design can be altered by changing the following features: length/diameter (L/D) ratio and compression ratio.

The L/D ratio is the ratio of the screw length to its outside diameter. L/D ratio ranges from 18:1 to 32:1, with 24:1 as the most common. As L/D ratio increases, residence time, shear, heat uniformity, and mixing increase (Painter and Coleman 2008). While the feed section controls the flow of resin through the barrel, the compression section is designed with an increase in screw diameter to build pressure and shear on the plastic as it is forced against the barrel wall. The combination of applied external heat and frictional heat causes the plastic to soften and melt. Screw compression is quantified by the compression ratio, the feed channel volume to meter channel volume ratio, which ranges from 2:1 to 4:1. As the compression ratio increases, shear and heat uniformity increase, but this heightens the potential to stress the polymer chains (Painter and Coleman 2008). The metering section delivers the molten polymer to the extruder die, which determines the profile of the gob of molten polymer. The pressure of the molten plastic before it enters the die ranges from 1000-5000 psi. The temperature zones and

screw speed of the extruder is dependent upon the melt properties of the material (Table 2.5).

Table 2.5: Processing temperatures for common plastics. (Adapted from Selke and Culter 2016).

Polymer	Processing Temperature (°C)
High Density Polyethylene	200-280
Low Density Polyethylene	150-315
Linear Low Density Polyethylene	190-250
Polypropylene	205-300
Polystyrene	180-260
Polyvinyl Chloride	180-260
Ethylene Vinyl Alcohol	160-210

Extruders are categorized into single or multi-screw extruders. Single screw extruders are the most commonly used extruder machines because of their simple design, ruggedness, and performance to cost ratio (Drobny 2014). Single screw extruders are primarily used for pumping, conveying, and forming polymeric melts. Compared to single screw extruders, twin screw extruders are more efficient in mixing ingredients such as additives, fillers, and liquids (Shrivastava 2018). Twin screw extruders are commonly used for biocomposite preparation for its good dispersion, however productivity decreases with fiber content because polymer fluidity decreases (Tanaka and Ito 2013). The most suitable machine for composite processing is dependent on the formulation, desired quality, and allowed costs. The mixing efficacy of single screw extruders can be improved with design modifications, but it will not be as effective as twin screw extruders. Supercritical CO_2 has been utilized as a mixing aid in clay-PP nanocomposite for single screw extrusion processing. Although the super critical CO_2 provided better clay exfoliation and dispersion, conventional twin screw extrusion without supercritical CO_2 still provided higher shear and better mixing of clay in the polymer matrix (Treece and Oberhauser 2007).

Once the biocomposite polymeric melt has been thoroughly melted and mixed via extrusion, the melt is cooled and pelletized and ready for further processing. Two commonly used processes for biocomposite manufacturing are compression molding and injection molding. Compression molding is accomplished by placing plastic granules into a mold to be formed using heat and pressure. A typical compression molding process is performed at a melting temperature of 350°F and pressure of 100 psi with a curing time of 3 minutes. Whereas injection molding is performed by injecting molten plastic into a mold. Successful injection molding requires specific melt temperature to ensure proper processing viscosity and pressure to prevent flashing.

There is a complex relationship between processing method, fiber loading, and fiber orientation on biocomposite mechanical properties. It has been concluded that with sufficient fiber length and elimination of voids would result in higher strength values of injection molded composites compared to compression molded composites due to enhanced fiber wettability, which results in better fiber/matrix adhesion (Graupner et al. 2016).

2.7 Instrumental analysis of polymers

The properties and characteristics of polymers are determined using standardized test methods by organizations such as the American Society for Testing and Materials (ASTM). ASTM methods measure mechanical and thermal properties, as well as to characterize the physical structure for materials and products. These analyses are used to both predict and evaluate performance.

2.7.1 Mechanical properties

Mechanical properties are physical properties that a material exhibits upon the application of forces. Tensile properties are measured using a Universal Testing Machine, which applies a constant rate of deformation using a load cell to measure and record the force required to cause deformation. Tensile testing produces a stress-strain curve, graphing the increase in length divided by the original length (strain) on the x-axis and the tensile load divided by the cross sectional area (stress) on the y-axis (Figure 2.7). Materials can be characterized as tough, brittle, hard, and soft depending on their mechanical properties (Table 2.6).

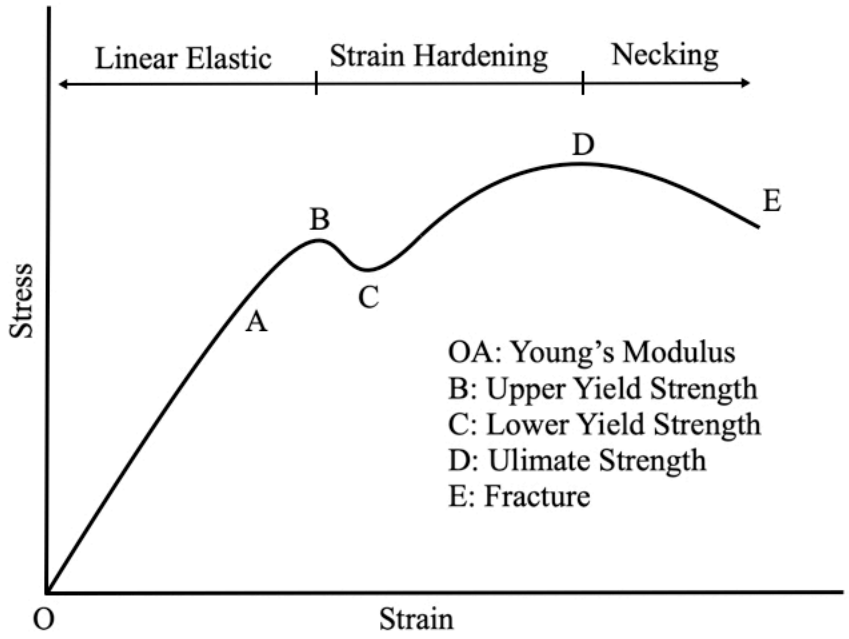

Figure 2.8: Typical stress-strain curve from tensile testing

The first stage of the stress strain is the linear elastic portion where the material exhibits an initial linear relationship between stress and strain. The slope of the linear portion of the stress-strain curve is known as *Young's modulus*. An increase in Young's modulus indicates that a higher amount of stress is required for a given amount of strain, which suggests the material is more rigid and has a higher resistance to bend or *flexural*

modulus. The *elastic limit* is the last point at which when applied stress is removed, the material returns to its original dimensions. After the elastic limit, the strain hardening stage begins with the *yield point*, the point at which the material will undergo permanent deformation when applied stress is removed. The *ultimate strength* and *ultimate elongation* are the highest stress the material can withstand before rupture and the strain at its break point, respectively. The region between the ultimate strength and fracture is the necking stage, which is identified when the local cross-sectional area becomes significantly smaller than the average.

Table 2.6: General characteristics of polymers according to their mechanical properties (Adapted from Selke and Culter 2016).

Type of Polymer	**Elastic Modulus**	**Yield Stress**	**Ultimate Strength**	**Elongation at Break**
Soft and weak	Low	Low	Low	Moderate
Soft and tough	Low	Low	Moderate	High
Brittle and hard	High	-	Moderate	Low
Hard and strong	High	High	High	Moderate
Hard and tough	High	High	High	High

2.7.2 Water absorption properties

Moisture absorption is the capacity of a polymer to absorb moisture from its environment. There are three mechanisms of water diffusion in polymeric composites (Dhakal et al. 2007). In the first mechanism water diffuses in between the micro gaps of polymer chains. The second mechanism involves the capillary transport of water into the gaps between fiber and matrix. The last mechanism is the transport of microcracks in the matrix due to fiber swelling. Absorbed water may affect materials' dimensions and mass and can extract water-soluble components, which results in a degradation of mechanical properties (Yang et al. 2006).

2.7.3 Physical structure

Microscopy is used to understand polymer topography and morphology. For example, the instrument can observe crystal growth and filler dispersion and can be used to understand structure-property relationships. Scanning electron microscopy (SEM) uses a low energy electron beam to scan the surface of the polymer. A variety of interactions between the electrons and sample are detected and processed. The three types of emitted signals are: secondary electrons, backscattered electrons, and characteristic x-rays. This information forms images of the material's microstructure and morphology.

2.7.4 Thermal properties

Thermal properties refer the behavior of materials in the presence of heat. Thermal stability is an important quality that affects the final quality and application of the material. For example, materials that require high heat stability are car dashboards and bathroom interiors. Thermal analyses provide fundamental information on molecular structure, crystallinity, and composition. Three crucial thermal analyses are thermogravimetric analysis (TGA), differential scanning calorimetry (DSC), and dynamic mechanical analysis (DMA). TGA continuously measures the mass of a sample over time as the temperature increases. The thermal property information collected from TGA includes water content, composition, and thermal degradation profile. DSC measures the heat flow through the sample compared to a reference to identify thermal transitions such as glass transition, melting, and crystallization. On a DSC curve, the glass transition temperature (T_g), crystallization temperature (T_c), and melting temperature (T_m) are represented by a step change, a big peak, and a big drop, respectively (Figure 2.9).

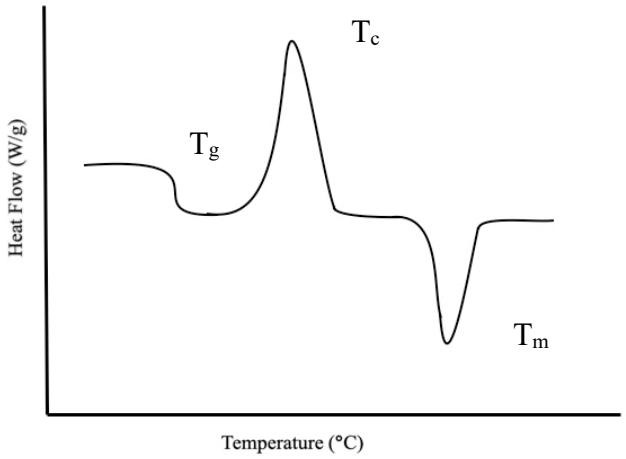

Figure 2.9: Example of a differential scanning calorimetry curve

2.8 Environmental issues of plastics

Plastic material is an integral part of our daily lives with an annual production of >380 million tons worldwide in 2015 (Ritchie and Roser 2018). Since its beginning in the early 1900's, plastics have been favored over natural materials because it is comparatively affordable and resistant to rot, chemicals, and deformation (Crespy et al. 2008). Plastic is an essential material across industries from consumer goods, food retailing, construction, transportation, textiles, among others. As the profits for chemical, oil, and plastic manufacturing rise, so does the volume and consumption of plastic around the world (Dauvergne 2018). In 2015, the United States generated 34.5 million tons of plastic and accounted for 13.1% of municipal solid waste (EPA 2019). The recycling rate in 2015 was 9.1% and 15.5% of plastic was combusted for energy recovery, however a large majority (75.4%) of plastic was landfilled (EPA 2019).

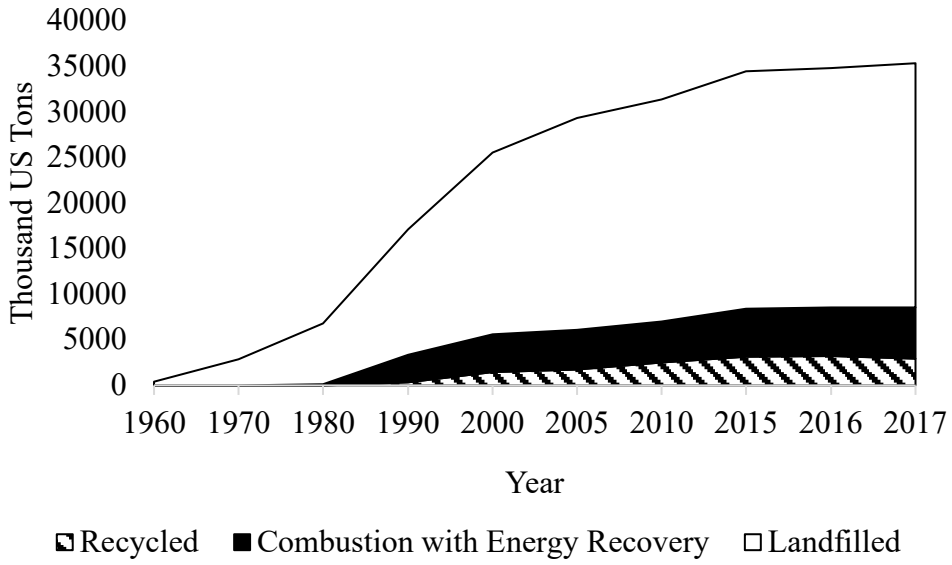

Figure 2.10: Municipal solid waste management in the United States (Adapted from EPA 2020c).

Plastics are becoming an environmental issue as commercial packaging is not biodegradable because of their high molecular weights and rigid structures which are not appropriate for organismal digestion, and because many plastics contain substituents that prevent biodegradation via the enzymatic fatty acid oxidation method (Klemchuk 1990). There is an estimated 150 million tons of plastic accumulated in the world's oceans and this number is expected to reach 250 million tons by 2025 (Jambeck et al. 2015). Plastic pollution raises issues effecting not only marine life but also food security, food safety, and human health (Gall and Thompson 2015; Eagle et al. 2016; Barboza et al. 2018; Dauvergne 2018). There is a growing global initiative towards reducing disposable plastics and transitioning towards a circular economy for plastic. In 2017, six major international companies pledged to "use 100% reusable, recyclable, or compostable packaging by 2025" and by late 2018 over 350 organizations signed up for this global commitment to eliminate plastic waste and pollution (EMAF 2018). This global initiative

has directed research towards improvements and innovations in green materials made from sustainable resources.

2.8.1 Biocomposite waste management

Bioplastics and biocomposites research has been done to create cost-effective, eco-friendly materials, however the introduction of these "green materials" introduced new issues regarding end of life solutions. Questions were raised concerning the risk of contamination, cost of separation, technical feasibility, and impact on recycled material quality without jeopardizing the current recycling system (Soroudi and Jakubowicz 2013). Currently, there are three methods of recycling for biocomposites: (1) mechanical recycling, (2) chemical recycling, and (3) thermal processing (Yang et al. 2012). Mechanical recycling, the most successful recycling method, remelts and remolds biocomposites through multiple extrusion and/or injection cycles. Mechanical recycling is favored for its ease of processing and parametric control (Badia et al. 2012). Chemical recycling dissolves the polymer matrix and separates the fibers from the matrix, while thermal processing recovers energy through incineration.

Sisal fiber biocomposites with a fiber loading of 30 wt% were successfully produced and mechanically recycled for several extrusion/injection cycles (Bourmaud and Baley 2007; Chaitanya et al. 2019). The tensile and flexural strength of the recycled sisal fiber-PLA biocomposites decreased by 20.9% and 21.2% respectively, up to the third recycle, beyond which a significant reduction was observed. The biocomposites also experienced a decrease in viscosity and glass transition temperature indicating chain scission and hydrolytic degradation. The recycling analyses suggested that the recycling process does not show a significant effect on the mechanical properties of the

biocomposites up to three cycles, which makes the recycled materials acceptable for low to medium-strength nonstructural applications.

Overall, recycling biocomposites while still conserving its mechanical properties are successful up to several reprocessing cycles. Multiple cycles may even enhance the interfacial adhesion between fillers and matrix, resulting in a reported increase in thermal stability in the reprocessed biocomposites (Beg and Pickering 2007). However, degradation will occur from repeated recycling cycles for reasons such as fiber length reduction and plastic polymer chain scission, which causes molecular weight to decrease and crystallinity to increase (Vilaplana et al. 2010).

The remaining waste-management practices include composting, incineration, and landfill. However, a Life Cycle Analysis (LCA) examining end of life scenarios for wood flour-PP and flax fiber-PLA biocomposites concluded that recycling is the most preferred scenario to avoid environmental impact because recycling reduces material production (Beigbeder et al. 2019). Composting is only feasibly if the composite contains a biodegradable polymer, but is still a viable option for eco-friendly waste management. Incineration and landfill are harmful to the environment with relatively high impacts on climate change, human toxicity, and freshwater ecotoxicity, with landfilling having a larger impact in each category. It is understood that current biocomposite recycling data is collected in polymer labs, and enhanced quality and reliable data is necessary to have a higher degree of credibility in the LCA results (Mansor et al. 2015). Although, the current waste stream of biocomposites is relatively small and has no effect on current recycling methods (Karpenja et al. 2013). In the future, the amount of green materials in

the waste stream may grow and will require further research to examine its effect on recycling.

CHAPTER 3 – MATERIALS AND METHODS

3.1 Materials

3.1.1 Peach flour

The peach stones were sourced from Del Monte Foods, Inc., a fruit processing facility located in Stanislaus, California and came from *Prunus* peaches harvested summer 2017. The peach stones were stored in the dark at refrigeration temperature until further processing.

Whole peach stones (endocarp and seed) were processed into flour using two different machines: a W Series Laboratory Scale Hammer Mill (Schutte Buffalo, SN: 6 08 0088) equipped with a dust collector (DCS370, Powertec, Waukegan, IL) and a Country Living Grain Mill equipped with a gearmotor (CM32D25VZ2A, Leeson, Orange, CA). Preliminary formulations contained peach stones processed with the hammer mill, whereas DOE formulations contained peach stones processed with the grain mill due to equipment complications. The hammer-milled peach stones were processed using mesh screen sizes 3/4", 1/8”, and 0.027” at 27-32 rotations per minute (rpm). The grain-milled peach stones were processed at maximum fineness at roughly 80 rpm (Figure 3.1). Regardless of how the flour was obtained, the peach flour (PF) was sieved through a pore size of 250 microns. The peach flour was stored in the dark at refrigeration temperature until further processing.

(a)  (b) 

Figure 3.1: Peach stones (a) pre-mill and (b) post-mill processing.

3.1.2 Plastic polymer resin

HDPE resin with a melt flow index of 0.085 g/min and density of 962 kg/m^3 was sourced from Dow Chemical Company (Elite 5960G, Midland, Missouri). PP resin was sourced from INEOS (League City, Texas). The coupling agent used in this work was MAH-g-HDPE Amplify GR 204 with a melt flow index of 12 g/min and density of 950 kg/m^3 supplied by Dow Chemical Company (GMID: 258420, Batch: D381HBORV, Midland, Missouri).

3.2 Proximate analysis of peach flour

The PF was dried in a convection oven (Despatch, Minneapolis, Minnesota) at 75°C for at least 16 hours prior to proximate analysis. Particle size of the ground peach pits was determined using a particle size analyzer (Coulter Particle Characterization LS230, ID: 29597, Indianapolis, ID). Moisture content of the PF was determined using a Q50 thermogravimetric analyzer (TA Instruments, SN: 0050-1879, New Castle, Delaware) by heating approximately 5 mg of sample to 600°C at a rate of 10°C/min. Ash content was determined using a muffle furnace (Barnstead International, Model: F62735, SN: 1276040267170, Dubuque, Iowa), which heated 5 g of sample to 600°C (McClements 2003). Ash content was calculated using Eq. 3.1.

$$\%Ash\ (Dry\ Basis)\ =\ \frac{M_{ash}}{M_{dry}}\ x\ 100 \tag{3.1}$$

Where:

M_{ash}= Mass of ashed sample in grams.
M_{dry}= Mass of original dried sample in grams.

Kjeldahl nitrogen was measured using a modified Kjeldahl method with a Kjeltec 8200 (FOSS, Eden Prairie, Minnesota) (Kjeldahl 1883). A ~1.0g sample of dried PF was added to a Kjeldahl tube with 2 Kjeltabs Cu catalyst tablets and 12ml of concentrated H_2SO_4. The exhaust manifold was placed on the tubes, which were then placed on the pre-heated block. The tubes were digested at 420°C for 60 minutes. After digestion, the tubes were moved off the manifold to cool to less than 100°C. Next, the sample goes through automated distillation with 50ml 40% w/v sodium hydroxide (NaOH) and 30ml boric acid (H_3BO_4). Finally, titrations were performed on the receiving solution and distilled PF samples with standard 0.10N hydrochloric acid (HCl) to a violet end-point. Kjeldahl nitrogen was calculated using Equation 3.2 with a factor value of 6.25.

$$\%Kjeldal\ Nitrogen\ =\ \frac{(V_s - V_b)\ x\ C\ x\ 1.4007}{W} \tag{3.2}$$

Where:

V_s= mL of standardized acid used to titrate sample.
V_b= mL of standardized acid used to titrate reagent blank.
C= Concentration in moles/L of the HCl solution used for titration.
W = Weight of sample in grams.

Lipid content was determined using a modified Soxhlet method with a Soxtec 2043 (FOSS, Eden Prairie, Minnesota) (AOAC 2000). A 2-3g sample of dried PF was placed in a dried cellulose thimble, which were placed on the condenser valve. Extraction cups with 30ml petroleum ether was clamped into the condensers. Next the automated

machine distilled the sample. After a 1 hour extraction, the extraction cups were cooled and weighed. Lipid content was measured using Equation 3.3.

$$\%Fat = \frac{W_3 - W_2}{W_1} \quad (3.3)$$

Where:

W_1= Sample weight in grams.
W_2= Extraction cup weight in grams.
W_3= Extraction cup + residue weight in grams.

Fiber analysis was done on the dried PF following the Van Soest method (Van Soest et al. 1991). Amylase neutral detergent fiber (aNDF) and acid detergent fiber (ADF) analyses were performed sequentially. Hemicellulose and cellulose contents were expressed as the difference of aNDF and ADF. Berzelius beakers (600 mL) containing 0.5 g of sample and 200 mL neutral detergent solution (Ankom, Macedon, New York) were refluxed, boiled and the vapors were re-condensed into the liquor, using a Labconco crude fiber apparatus (Kansas City, Missouri) for 5 min before 2 mL of heat stable α-amylase was added. After the α-amylase addition, the contents of the beaker were refluxed for an additional 60 min. The NDF solution and residue were vacuum filtered into a fritted crucible (50 mL, coarse porosity, 40-60 μm). When the only residue was left in the crucible, 50 mL of boiling deionized (DI) water and 2 mL of α-amylase were added and allowed to set for 1 min before being filtered. The samples were then soaked in 30 mL of acetone before being filtered. After being filtered, the crucible was once again soaked in 30 mL of acetone and filtered once again. The crucibles were placed under a fume hood overnight and then placed in a 105 °C drying oven (Blue M, Blue Island, Illinois) for 24 h before ADF analysis. The only modifications for the ADF procedure were that α-amylase was not used, and the neutral detergent solution was replaced with

acid detergent solution. The samples were then dried for 24 h at 105 °C. aNDF% and ADF% were calculated using Eq 3.4 and 3.5, respectively.

$$aNDF\% = \frac{W_3 - W_1}{W_2 x \frac{Lab\ \%DM}{100}}\ x\ 100 \tag{3.4}$$

$$ADF\% = \frac{W_4 - W_1}{W_2 x \frac{Lab\ \%DM}{100}}\ x\ 100 \tag{3.5}$$

Where:

W_1= Mass of crucible in grams.
W_2= Mass of sample in grams.
W_3= Mass of crucible + aNDF residue in grams.
W_4= Mass of crucible + ADF residue in grams.

3.3 Biocomposite preparation

Various biocomposites were created with different PF loadings, compatibilizer resin (CR) concentrations, and polyolefin matrices. The PF, CR, and polymer resin were fed into a C. W. Brabender twin screw extruder (Type: 15-47-000, SN: CO8-147/B, Hackensack, New Jersey) at a rotary speed of 70 rpm with temperature zones at 151, 170, and 180°C for HDPE and 171, 190, and 200°C for PP. As the gobs were extruded, they were manually flattened and collected into a bucket. The gobs were cooled to room temperature at ambient conditions then pelletized using a granulator (Ball and Jewell-Sterlco, Model: G68, SN: 96H0064, Milwaukee, Wisconsin) with a mesh screen size of ¼ inch.

Modification for the masterbatch process was that the PF-polyolefin biocomposite granules were passed through the twin screw extruder for a second time under the same conditions. The gobs were again flattened, cooled, and pelletized.

The granules were converted into a film using a compression molder (PhiHydraulics, Model: B354H-X1-4A-6-8-14, SN: 90-9-017, City of Industry,

California). The granules were spread evenly on curing paper and placed between two aluminum plates (Figure 3.2). The granules were then pressed at 171°C and 25-30 tons of pressure for 60 seconds (Figure 3.3). The film was kept between the curing paper until it was cool to the touch, then it was removed from the paper and cooled to room temperature. The films were stored and conditioned in a Darwin Chamber (Model: PH09-DA, SN: 12171895, St. Louis, Missouri) at 25°C and 50% RH for 24 hours prior to instrumental analysis.

(a)  (b) 

Figure 3.2: Peach flour -high-density polyethylene biocomposite granules (a) spread on curing paper and (b) placed in between two aluminum plates

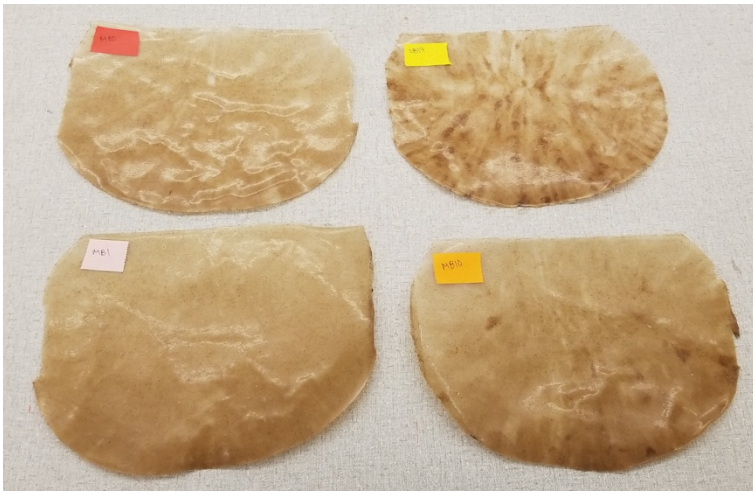

Figure 3.3: Peach flour -high-density polyethylene biocomposites post-compression molding process

3.4 Preliminary experiments for design of experiment

The goal of the preliminary experiment was to determine factor levels for the design of experiment. Preliminary formulations were done with increasing PF and CR concentrations (Table 3.1). Preliminary experiments were performed in preparation for a design of experiment (DOE) (1) to narrow PF and CR concentration ranges and (2) to determine whether single or masterbatch processing produced stronger biocomposite. Preliminary levels of PF were based on previous natural fiber-filled biocomposite studies (Kaboorani 2010; Ayrilmis et al. 2011; Banat 2019). The preliminary CR levels were according to the recommended usage level of Amplify GR 204.

Table 3.1: Preliminary formulations of peach flour -high-density polyethylene biocomposites

Composition Code	% HDPE	% MAH-g-HDPE	% Peach Flour
SB 0	95	0	5
SB 1	94	1	5
SB 3	92	3	5
SB 5	90	5	5
SB 10	85	10	5
SB 15	80	15	5
SB 17	78	17	5
MB 0	95	0	5
MB 1	94	1	5
MB 3	92	3	5
MB 5	90	5	5
MB 10	85	10	5
PF 10	77	15.3	7.7
PF 20	62.5	25	12.5
PF 30	52.7	31.5	15.8
PF 40	45.4	36.4	18.2
PF 50	40	40	20

A formulation processed through the extruder once was labeled as Single Batch (SB) and a formulation processed twice was labeled as Masterbatch (MB).

3.5 Response surface methodology to optimize biocomposite formulation

Response surface methodology was used to optimize the biocomposites formulations for maximum tensile strength. The DOE was developed using JMP 14.0

(SAS Institute, Cary, North Carolina). Three variables were selected for the central composite design (CCD): PF loading, CR concentration, and polyolefin matrix. The levels of PF and CR were based on the preliminary experiments. The DOE consisted of two identical designs of 15 runs, each with replicates at the high and low levels (Table 3.2). The extremes were replicated rather than the center point to offset variability at those levels. The difference between the designs was the polyolefin matrix, one design used PP and the other used HDPE. Additionally, the run order of each design was randomized to account for environmental variability and experimental bias.

Table 3.2: Peach flour -polyolefin biocomposite compositions

Code PP- or PE-	% PF	% CR	% PP or PE
1	2.5	5	92.5
2	2.5	5	92.5
3	5	5	90
4	10	5	85
5	10	5	85
6	10	5	85
7	2.5	10	87.5
8	5	10	85
9	10	10	80
10	2.5	20	77.5
11	2.5	20	77.5
12	5	20	75
13	10	20	70
14	10	20	70
15	10	20	70

3.6 Instrumental analysis

3.6.1. Mechanical property analysis using a universal testing machine

The thickness of the film was measured using a micrometer (Messmer Buchel, SN: 103012-01, New Castle, Delaware). Film samples were cut into 1 inch x ~5 inch rectangles using a precision sample cutter (JDC, Model: 25, SN: 29323, Philadelphia,

Pennsylvania) for mechanical performance testing and analyzed with a universal testing machine (Testometric, M350-5, Rochdale, England). Both ends of the rectangles were wrapped in laboratory tape (Figure 3.4). Tensile testing was performed to measure the force required to rupture the material. Tensile testing followed ASTM D882 with a crosshead speed of 25 in/min and 500 kg load (Testometric, 26100, Rochdale, England).

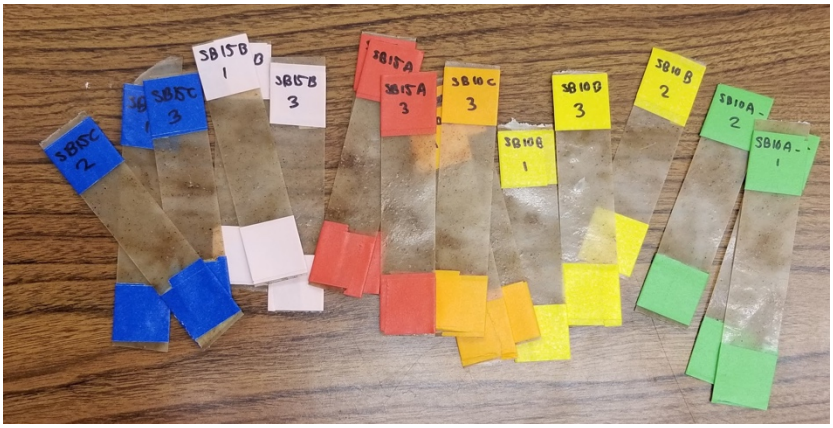

Figure 3.4: Peach flour -high-density polyethylene biocomposite samples for tensile testing

3.6.2 Thermal property analysis using thermogravimetric analyzer and differential scanning calorimeter

Thermal degradation profiles of the PF and biocomposites were determined using a Q50 thermogravimetric analyzer (TA Instruments, SN: 0050-1879, New Castle, Delaware) by heating approximately 5-6 mg of sample to 600°C at a rate of 10°C/min. This measurement provided information about moisture content, degradation temperature, and composition.

Differential Scanning Calorimetry (DSC) analysis was carried out using a TA Instrument, DSC Q 2000 (SN: 2000-2991, New Castle, Delaware) equipped with a Refrigerated Cooling System 90 (SN: RCS91-5002) on a 5–6 mg sample. Each sample was scanned using a "Heat, Cool, Heat" procedure under a nitrogen atmosphere (Table

3.3). DSC was used to study thermal transitions and phase changes such as melting, crystallization, and glass transition temperatures.

Table 3.3: Differential scanning calorimetry heating procedure

Cycle	**Ramp Rate (**° C/min)	**Temperatures (° C)**
1	10	Heat from 25 - 200
2	10	Cool from 200 - -90
3	10	Heat from -90 - 200

Crystallinity was calculated using equation 3.1 where ΔH^{exp} is the experimental heat of fusion, ΔH° is the standard enthalpy of fusion, and w_f is the weight fraction of the relevant polymer (Kuzmanović et al. 2018).

$$X_c = \frac{\Delta H^{exp}}{\Delta H^{\circ} w_f} \tag{3.6}$$

Where:

ΔH^{exp}= Experimental heat of fusion
ΔH° = Standard enthalpy of fusion
w_f= Weight fraction of the relevant polymer

3.6.3 Physical property analysis using ASTM D570 for water absorption

The water absorption of the PF-polyolefin biocomposites was measured using ASTM D570. Film samples (n=1) were cut into 1inch x 1inch squares and dried in an oven at 50°C for 24 hours. Upon cooling, the samples were weighed. The material was then submerged in water at 23°C for 24 hours. Samples were removed, patted dry with a dry cloth, and weighed. Water absorption was recorded as a percent increase in weight due to water uptake.

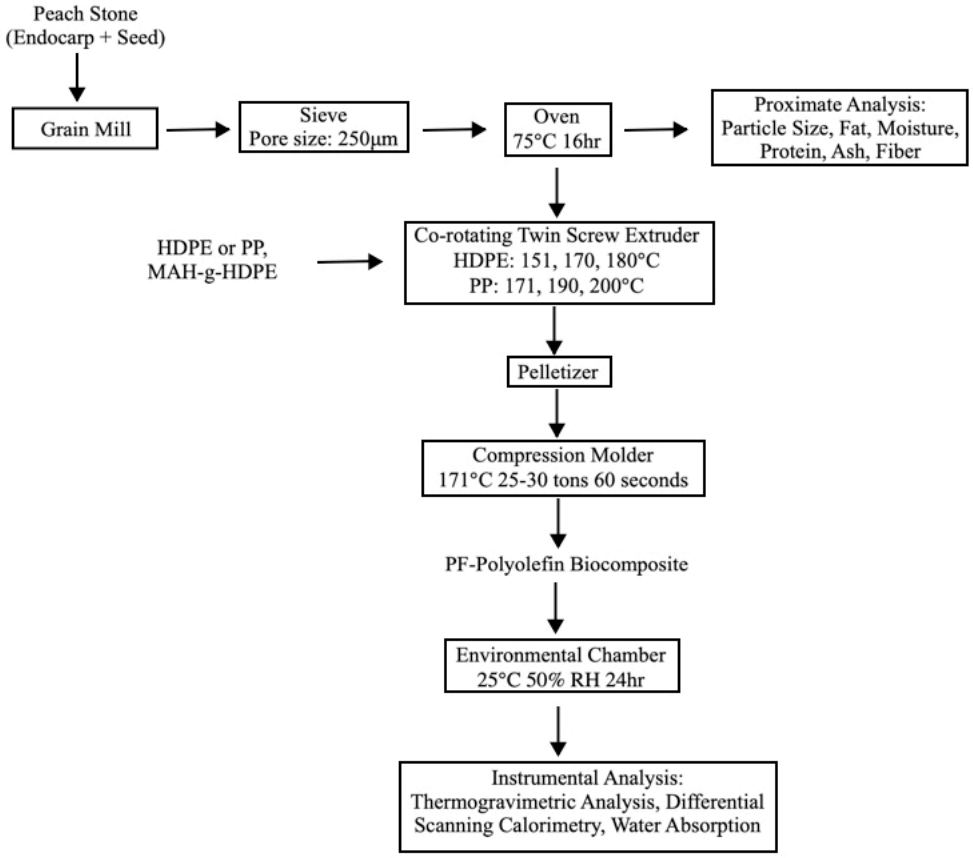

Figure 3.5: Process flow diagram for a peach flour -polyolefin biocomposite

3.7 Statistical analysis

Average values were reported out of 5 measurements for mechanical analysis. Thermal and water absorption analyses were not replicated (n=1) due to COVID-19 limitations. JMP 14 statistical software (SAS Institute Inc., Cary, NC) was used for the one-way analysis of variance (ANOVA) and to perform Tukey's Honest Significant Different (HSD) test with a critical significance level of 0.05. The RSM was applied for mechanical property and water absorption property analyses. The RSM used an equation to predict the response value by varying factor levels. Response surface plots were used to understand PF-CR interactions and their effect on measured responses.

CHAPTER 4 – RESULTS AND DISCUSSION

4.1 Proximate analysis of peach flour

The PF was analyzed for moisture, protein, fat, ash, and fiber content to understand its effect on composite properties (Table 4.1). The moisture (3.3%wt.), ash (1.6%wt.), and fiber (62.1%wt.) contents were comparable to the ones reported in the literature. Fruits contain natural minerals such as calcium, magnesium, zinc, iron, and potassium, which make-up their ash content (Torrens Zaragozá 2015). The ash content of fruit seeds generally ranges from 2.62-5.90% (Awotedu et al. 2020). The stones of stone fruits such as peach and apricot contain high energy and low ash contents <2.0%, which make them suitable for use as solid fuel to provide heat (Arvelakis et al. 2005; Ordoudi et al. 2018). The relatively low ash content of natural fibers has minimal effect on the performance properties of biocomposites (Singh et al. 2019).

We determined the combined amount of lignin and cellulose to be 62% db. Previous research has established that peaches and coconuts contain more lignin than other drupes (olives, black walnuts), with values upwards of 50% db (Mendu et al. 2011; Dardick and Callahan 2014). In contrast, drupes contain an average of 23% cellulose, a relatively low value compared to switch grass and woody crops, which range from 30-45% (Mendu et al. 2011). A high strength biocomposite would require a high-cellulose-fiber because cellulose's high aspect ratio and percent crystallinity can efficiently transfer stress and resist high impact (Liu et al. 2014). A high lignin content is beneficial for enhancing thermal stability and dispersion, and reducing hydrophilicity (Yang et al. 2019). Lignin increases thermal stability because it contains a complex phenylpropanoid unit with aromatic phenyl groups (Ghozali et al. 2017).

Table 4.1: Comparison of experimental and literature values for the proximate analysis of whole peach stones (endocarp and seed)

Analysis	Experimental (%wt.)[1]	Literature (%wt.)[1]	Source
Moisture	3.3 ± 0.9	4.77	Kaynak et al. 2005
Protein	30.5 ± 2.1	17-28[2]	Rahma and El-Aal 1988; Pelentir et al. 2011
Fat	8.9 ± 1.3	42-55[2]	Kamel and Kakuda 1992; Rahma and El-Aal 1988
Ash	1.6 ± 0.1	1.53	Kaynak et al. 2005
Fiber[3]	62.1 ± 0.4	67.2	Mendu et al. 2011

[1]Dry basis weight
[2]Values taken from peach seed analysis
[3]Lignin and cellulose

Protein content was higher than reported in the literature by ~44%, and fat content was lower by ~89%. Our values were obtained from the whole peach stone (seed and endocarp), whereas protein and fat literature values examined the peach seed only, which explained the discrepancy. The higher fat content reported in the literature can be due to the fact that the seed is rich in lipids and the woody endocarp is not, which most likely lead to the lower fat content in the values obtained in our study. The lower protein content of the peach seed (i.e., reported in the literature) can be explained by the fact that peach's woody endocarp likely contains structural protein in its cell walls (Bao et al. 1992).

As previously mentioned, fiber geometry is a highly influential factor in determining mechanical properties. Wood flour particles for composite applications range from 100-300 μm as the mechanical properties of composites increase with decreased particle size (Thomas et al. 2013; Zykova et al. 2015). The pre-ground peach stones were processed via a grain mill to create the PF. The mill's burrs were on the lowest setting and the flour was sieved to minimize particle size variability. The final PF particle size averaged 194.6 ± 102.5 μm and its particle size distribution is displayed in Figure 4.1.

The large standard deviation was attributed to the mill, which was designed with a burr grinding mechanism. This mechanism is highly variable because the fineness setting is determined by the distance between the two revolving burrs, which is set by the user. A grinding mechanism with a porous screen could produce a flour with smaller distribution because it eliminates human variability. Additionally, high distribution is common in composite research as a previous study stated that ~70% of particles ranged from 212-600 μm (Rosa et al. 2009; Sharma and Verma 2016).

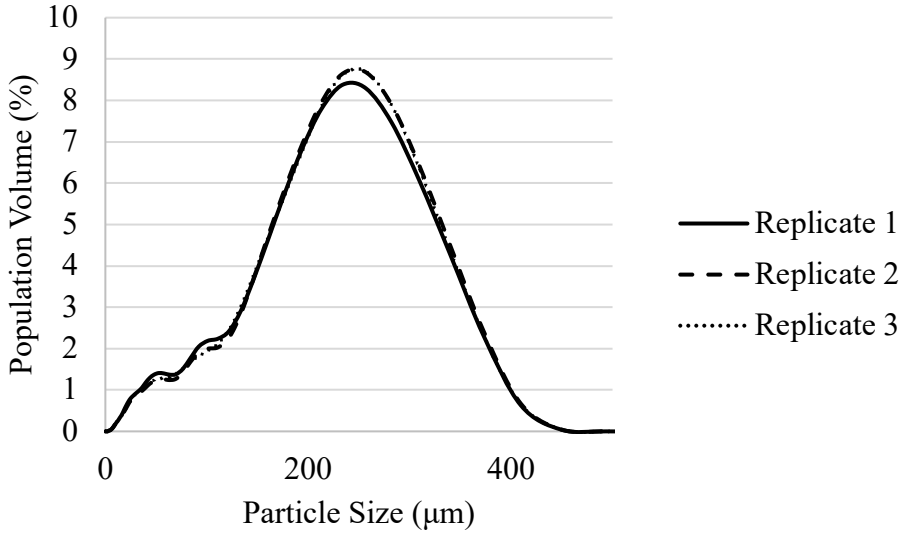

Figure 4.1: Particle size distribution of peach flour processed via grain mill

The thermal degradation profile of the PF was examined to understand its thermal stability, which could influence the final material's processing method and capabilities. The PF displayed an onset of thermal degradation at 160°C and a thermal degradation temperature (T_d) of ~220°C. The derivative weight profile displayed three inflection points: 202, 275, and 340°C (Figure 4.2). The three peaks were representative of the T_d values of hemicellulose, cellulose, and lignin, respectively (Yang et al. 2005).

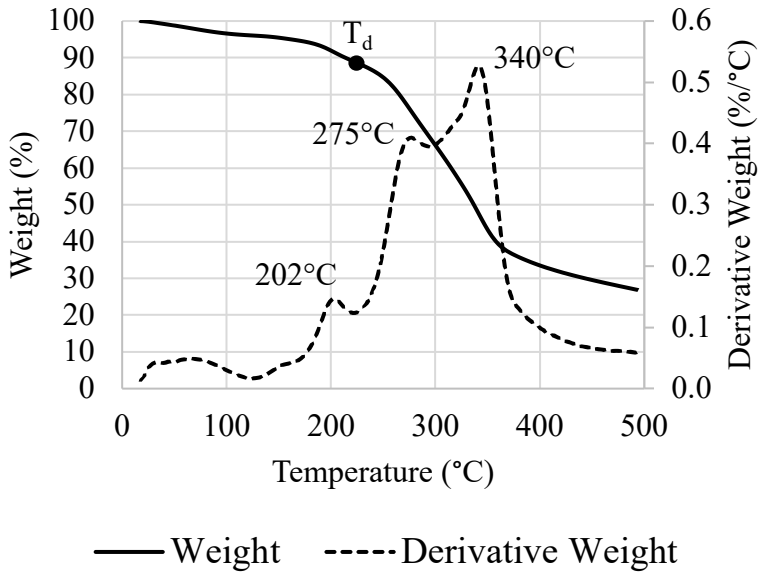

Figure 4.2: Thermogravimetric analysis thermogram of peach flour. The solid line represents the weight loss as temperature increases.

The peaks of the derivative weight profile represent the temperatures that experienced the most weight loss.

4.2 Preliminary tests: Understanding ingredient functionality

A preliminary experiment was performed to understand individual effects of each variable and narrow test variables and levels for the design of experiment. The experiment explored the effects of CR loading, PF loading, masterbatch processing, and polyolefin matrix.

4.2.1 Compatibilizer resin concentration

Understanding the effect of CR concentration is fundamental in optimizing the tensile strength of the final composite. The effect of CR concentration was studied by increasing its %weight concentration while maintaining a constant %weight of PF; the remaining percentage was made of HDPE resin. Coupling agent concentration requires optimization to produce an ideal composite. A concentration that is too low may not provide enough bonding strength between the natural fiber and polymer matrix, while too high concentration may cause fiber particles to aggregate (Liu et al. 2002). The optimal

concentration of the coupling agent capable of enhancing mechanical properties varies with each coupling agent-natural fiber pair. For example, previous studies that aimed to improve mechanical properties optimized an Argan nut shell-PP biocomposite with 8.0%wt. styrene–(ethylene–butene)–styrene-g-PP and a palm fiber-PP biocomposite with 2%wt. MAH-g-PP (Khalid et al. 2006; Essabir et al. 2016). The ratio of fiber to the coupling agent is another method of describing the required amount of copolymer (El-Sabbagh 2014). A study investigating the mechanical properties of flax-PP biocomposites utilized a MAH-g-PP:flax ratio of 1:10 by weight (Bos et al. 2006).

Figure 4.3 displays the effect of compatibilizer concentration on the tensile strength of PF-HDPE biocomposites with 5%wt. PF. The results showed an increase in tensile strength up to 10%wt. of CR. A 5% PF-HDPE biocomposite formulation with 10% CR was of nonsignificant difference with the HDPE control (Figure 4.3). According to the test result a 2:1 CR:PF ratio was considered the optimized formulation to produce a high strength PF-biocomposite.

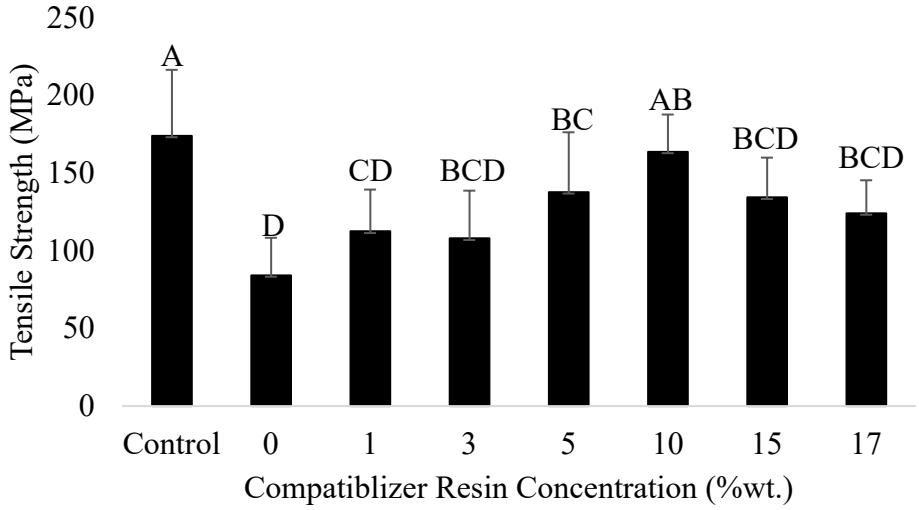

Figure 4.3: The effect of compatibilizer resin concentration on the tensile strength of peach flour -high-density polyethylene composites with 5%wt. peach flour. Different letters within a group indicate significant differences.

4.2.2 Masterbatch processing

A masterbatch is a pre-dispersed mixture of one or more additives in a resin. The masterbatch processing method can minimize exposure to hazardous additives and can enhance performance properties through improved dispersion. Masterbatch processing allows for longer residence time, which provides more time for shear forces to exfoliate filler particles between polymer chains and increase CR activity (Eteläaho et al. 2009). In this experiment, a masterbatch was created by processing the PF-HDPE composite twice through the extruder to ensure proper dispersion of PF and CR additives.

A formulation processed through the extruder once was labeled as "Single Batch". The effect of single and masterbatch processing is displayed in Figure 4.4. Pairs with an asterisk (*) identifies formulations that have significantly different single and masterbatch tensile strengths. There was no significant difference in 4 of 6 formulations investigated and those that were significantly different did not display a trend (Figure 4.4). Therefore, single batch processing was practiced for the remainder of the experiment. Masterbatch processing has been found to improve particle dispersion, but had weaker interactions than direct additive addition (Gu et al. 2015). The weaker bonds may be due to the increased residence time in the extruder, which can thermally degrade the biocomposite structure. The degradation mechanism of biocomposites has not been sufficiently explored, however it is well-established that exposure to high temperatures causes polymer degradation via four general mechanisms: chain scission, cross-linking, side-chain elimination, and side-chain cyclization (Beyler and Hirschler 2002; Niang et al. 2018). In application to our research study, HDPE degradation involves both chain

scission and recombination to produce cross-linked structures, while PP degradation involves primarily chain scission resulting in a lower molecular weight (Qian et al. 2011).

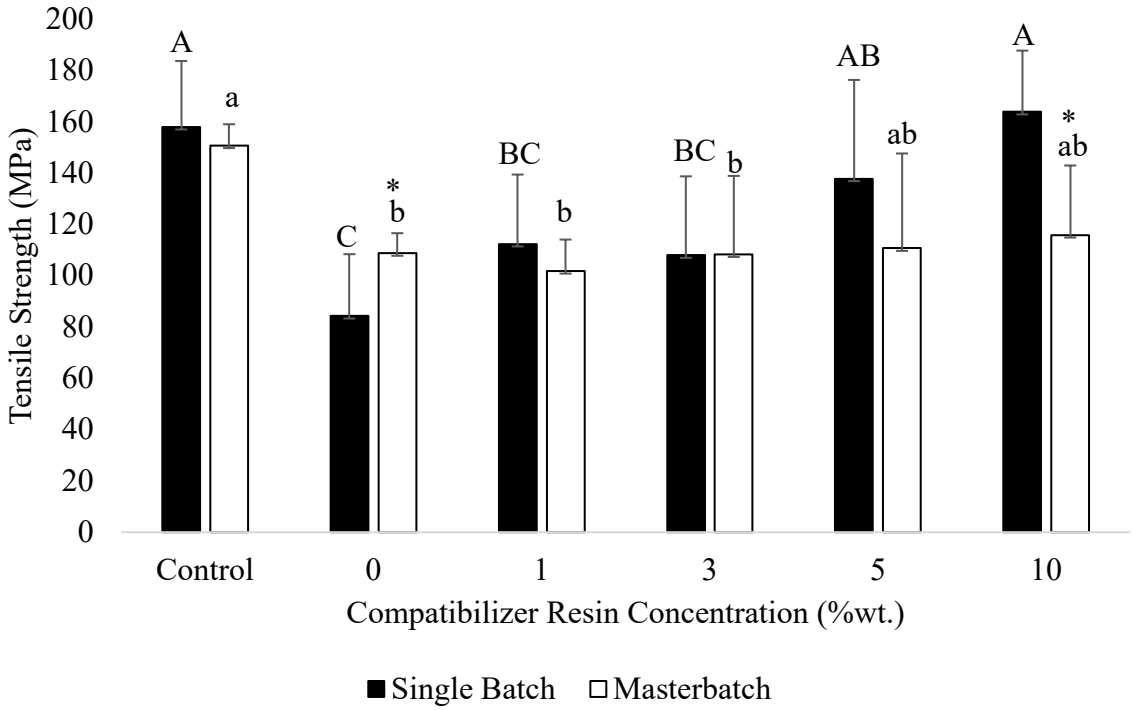

Figure 4.4: Effect of masterbatch processing on the tensile strength of virgin high-density polyethylene (Control) and peach flour -high-density polyethylene composites with 5%wt. peach flour and varying compatibilizer resin concentration.
Different letters within a group indicates significant differences; capitalized letters identify single batch formulations and lower-case letters identify masterbatch formulations. An asterisk (*) identifies formulations that have significantly different single batch and masterbatch tensile strengths.

4.2.3 Peach flour loading

Peach flour was compounded into an HDPE matrix at the following levels: 0, 5, 10, 20, 30, 40, and 50% with a 2:1 ratio of CR:PF. The additives (PF and CR) were added as a percentage of the amount of polyolefin resin. For example, a polyolefin resin amount of 100 g with 20% PF would include 20 g PF and 40 g CR. Formulations of up to 20%wt. PF were repeated with a PP matrix. The HDPE and PP composites with 5% PF were significantly stronger from their respective formulations with PF loadings of 10%

and higher (Figure 4.5). An optimized filler loading leads to higher tensile strength because of efficient stress transfer between the filler and matrix (Huda et al. 2008). While a high fiber loading leads to concentrated areas of stress and accelerated sample break (Tawakkal et al. 2012). Beyond 5% PF, polymer movement may be restricted and cause insufficient filling of the natural fibers into the polymer matrix (Han et al. 2006). Since biocomposites with 5% PF loading were significantly stronger than the higher PF loadings and displayed strength comparable to their respective controls, the DOE levels for PF loading ranged from 2.5-10% PF. These levels allowed us to explore interactions above and below the optimized PF load that enhance and worsen the biocomposite's performance.

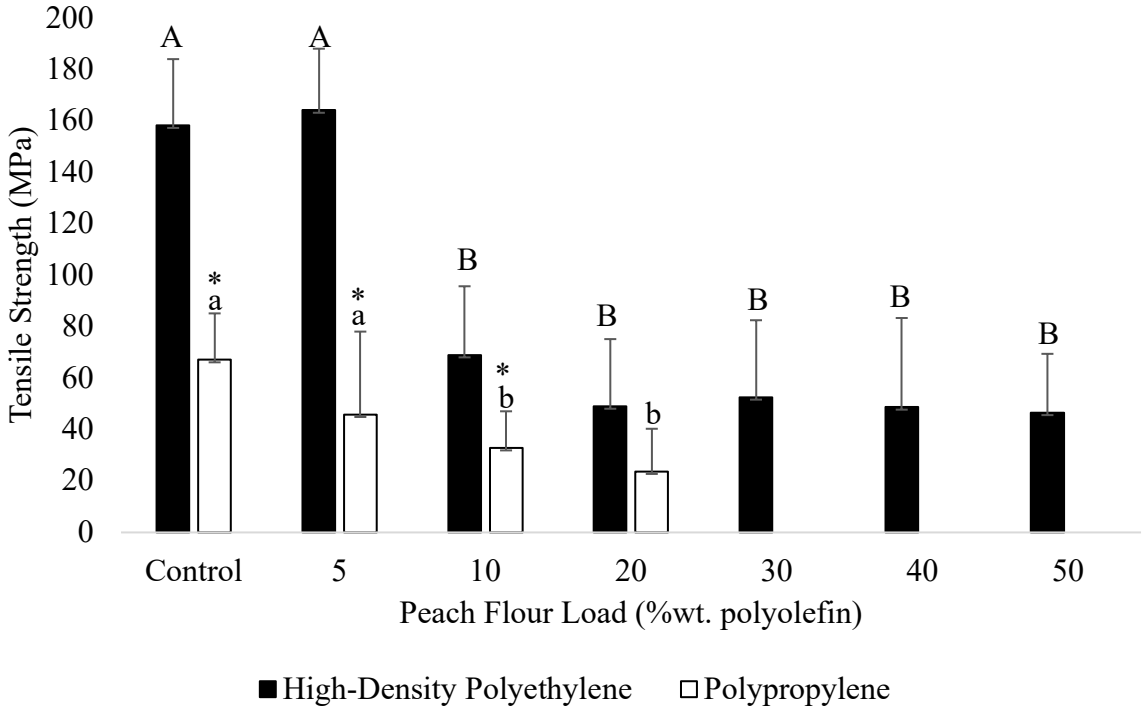

Figure 4.5: Effect of increased peach flour load on the tensile strength of peach flour - high-density polyethylene and peach flour -polypropylene composites with a 2:1 ratio of compatibilizer resin: peach flour.
[A-B] Different letters within a group indicate significant differences (for high-density polyethylene)

[a-b] Different letters within a group indicate significant differences (for polypropylene)
*Identifies formulations that have significantly different high-density polyethylene and polypropylene tensile strengths.

The effect of polymer matrices (HDPE versus PP) was examined to compare additive compatibility and determine which matrix could produce a stronger biocomposite. Figure 4.5 displays the effect of PF load on the tensile strength of both PF-HDPE and PF-PP biocomposites. An asterisk identifies formulations with significantly different HDPE and PP tensile strengths. PF-HDPE biocomposites with 5 and 10% PF loading were significantly stronger than their PF-PP counterparts (Figure 4.5). This result was expected because virgin HDPE control was significantly stronger than the virgin PP control (Figure 4.5).

4.3 Effect of peach flour, compatibilizer resin, and polyolefin on mechanical, thermal, and physico-mechanical properties of peach flour-polyolefin biocomposites

A central composite design (CCD) was used to determine the effect of PF loading, CR loading, and polyolefin matrix on biocomposite mechanical, thermal, and physico-mechanical properties and to optimize the biocomposite formulation for maximum tensile strength. Design factors were: PF (2.5, 5, 10%), CR (5, 10, 20%) and polyolefin matrix (HDPE or PP). Factor levels were based on preliminary results discussed in section 4.2. Response surface models were created using regression models that best predicted the response. Model adequacy was evaluated using residual analysis for normal distribution and unequal variance.

Figures 4.6 and 4.7 display the effect of PF and CR contents on tensile strength of HDPE and PP biocomposites created for the DOE. Both matrices resulted in high variability, which was likely due to poor particle dispersion. The formulations with 5% CR generally produced stronger biocomposites than those with 10 and 20% CR. This

trend lead us to focus on formulations with 5% CR and 2.5-10% PF loading for our discussion. Although the HDPE formulation with 20% CR and 2.5% PF resulted in comparable tensile strength with the formulation with 5% CR and 2.5% PF, the lower CR concentration was focused on because it would be more economical to utilize a lower CR concentration.

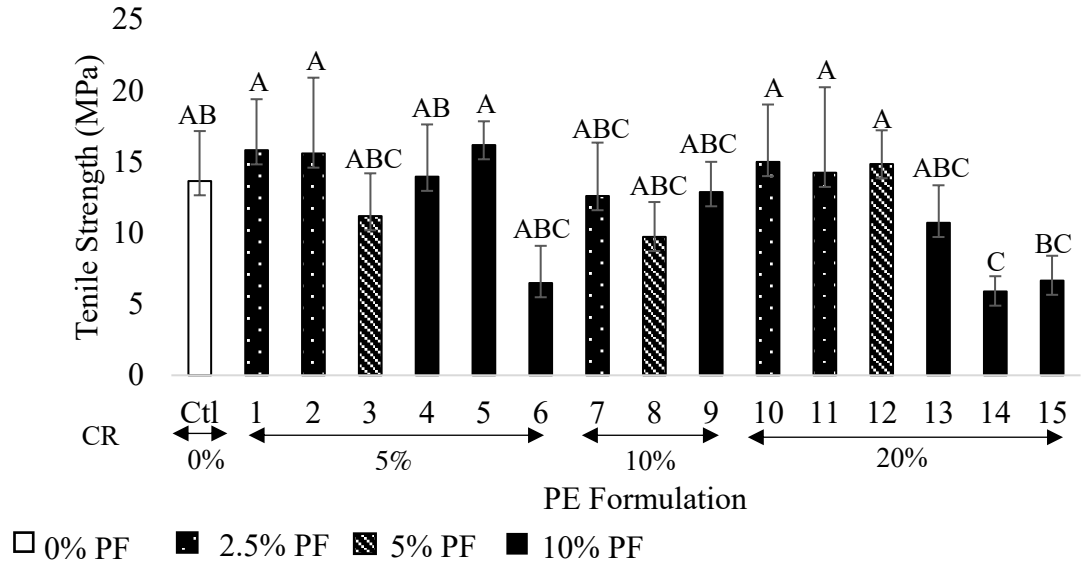

Figure 4.6: Tensile strength values for all high-density polyethylene design of experiment formulations.

The legend describes the peach flour content and the arrows under the X-axis describe the compatibilizer resin content of each formulation. Different letters within a group indicate significant differences.

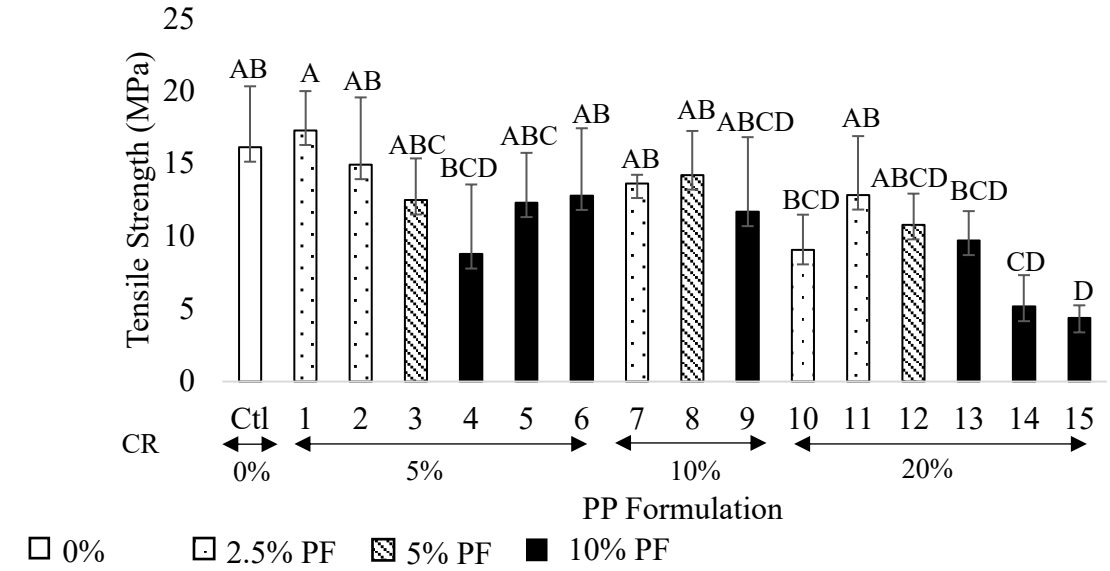

Figure 4.7: Tensile strength values for all polypropylene design of experiment formulations.

The legend describes the peach flour content and the arrows under the X-axis describe the compatibilizer resin content of each formulation. Different letters within a group indicate significant differences.

4.3.1 Mechanical properties

4.3.1.1 Tensile strength

The effect of PF loading on the tensile strength of polyolefin composites with 5% CR is displayed in Table 4.2. The addition of PF made a significant difference on biocomposite tensile strength for two formulations, PP5 and PP10 (Table 4.2). However, there was no significant difference between the two concentrations. With PE, adding PF did not have any significant impact on tensile strength.

It can be seen that the full regression model had only one significant factor, PF (P=0.001, α=0.05) (Table 4.3). The model was reduced to the linear effects of PF and CR and their interaction. The plastic type resulted in a P value of 0.95, indicating it was not significant and was taken out of the model (α=0.05). Although the interaction of PF*CR was not significant, the linear effects were highly significant and justified the interaction

being included in the model. The PF*CR interaction also increased the R^2(adj) value by 4.2% compared to a model with only PF and CR. The proposed model has an R^2(adj) value of 48.25%. The surface plots reflected the reduced model (Figure 4.8). The reduced regression formula was represented by the following equation:

$$TS = 17.34 + -0.51PF + -0.19CR + [(CR-11.25)*((PF-6.09)*-0.03)]$$

Table 4.2: Effect of peach flour (PF) loading on tensile strength of high-density polyethylene (PE) and polypropylene (PP) composites with 5% compatibilizer resin. Different letters within a group indicate significant differences.

Formulation		**Tensile Strength (MPa)**	
Polyolefin	**PF %wt. db**	**Average**	**Standard Deviation**
PP	Control	17.6^{AB}	3.1
	2.5	18.2^{A}	1.5
	5.0	11.4^{C}	1.5
	10.0	14.5^{BC}	2.1
PE	Control	14.9^{A}	2.6
	2.5	16.2^{A}	2.9
	5.0	12.0^{A}	2.7
	10.0	14.7^{A}	3.1

The formula predicted that PF and CR would only decrease tensile strength. However, PP and PE formulations with 2.5%PF increased tensile strength by 3% and 8%, respectively, compared to their controls (Table 4.2). Beyond 2.5% PF loading the tensile strength displayed a decrease with PF. This suggested a low PF filler loading is capable of producing a biocomposite of comparable strength to a neat polyolefin.

Table 4.3: Estimated variance analysis for the tensile strength of peach flour -polyolefin biocomposites (α=0.05)

Source	P Values	
	Full Model	Reduced Model
PF	0.00124	0.00031
CR	0.06164	0.00520
Plastic	0.94838	-
PF*PF	0.82588	-
CR*CR	0.75537	-
PF*CR	0.16702	0.07737
Plastic*CR	0.35270	-
Plastic*PF	0.72867	-
CR*CR*Plastic	0.71086	-
PF*PF*Plastic	0.95495	-

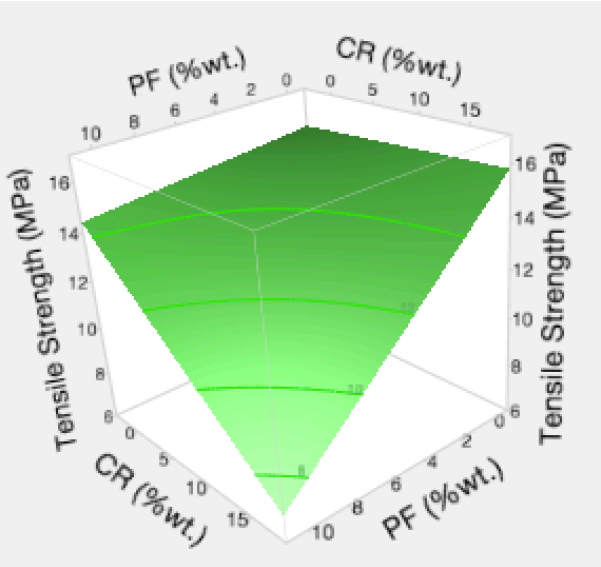

Figure 4.8: Response surface plot for the tensile strength of peach flour-polyolefin biocomposites as a function of peach flour (PF) and compatibilizer resin (CR)

The decrease in strength was an indication of incompatibility between phases. At high levels of PF and CR, the tensile strength was at its lowest for both PP and PE composites (Figure 4.8). Incompatibility between the CR and PP was evident in physical holes formed on the composite PP film compared to the PE film (Figures 4.9 and 4.10). It was also be seen that formulations with higher CR loading (Figure 4.10b) had more and larger holes than those with lower loadings (Figure 4.9b).

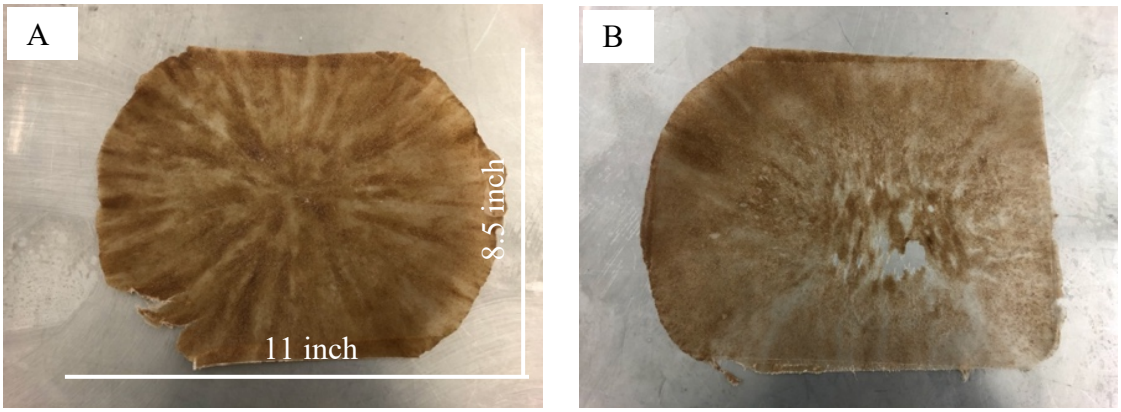

Figure 4.9: Images of films made with 10% peach flour and 10% compatibilizer resin in (a) high-density polyethylene and (b) polypropylene peach flour -filled biocomposites.

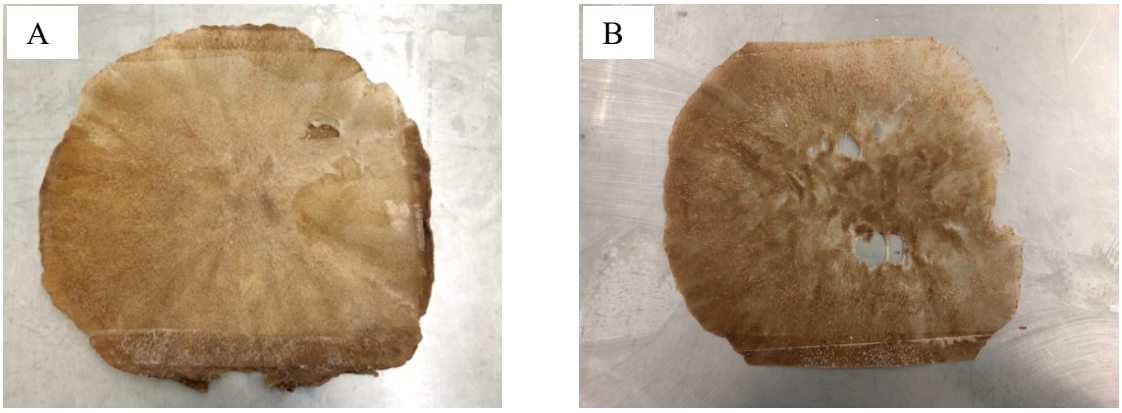

Figure 4.10: Images of films made with 10% peach flour and 20% compatibilizer resin in (a) high-density polyethylene and (b) polypropylene peach flour -filled biocomposites.

It has been established that biocomposite mechanical strength depends on three factors: (1) strength and modulus of natural fibers, (2) strength and toughness of the matrix, and (3) the effectiveness of stress transfer from fiber-matrix interfaces (Tragoonwichian et al. 2007). It can be assumed that the matrices' performance properties were unaffected because the processing temperatures utilized were below the common processing temperatures for HDPE and PP, which are 200-280°C and 205-300°C, respectively (Selke and Culter 2016; Zhu et al. 2019). Similar to our research study, an apricot shell-HDPE biocomposite with 30% filler loading resulted in a 28.2% decrease in tensile strength compared to neat HDPE (Essabir et al. 2014). Since there was

no significant increase in tensile strength with PF addition in our experiment, these results suggested that PF and potentially all stone fruits have poor mechanical properties or have a composition unsuitable for reinforcing polymer matrices (Zhu et al. 2019). This statement should be confirmed through physical and mechanical property tests on the PF (Djafari Petroudy 2017). Additionally, the overall decrease in tensile strength with CR and >2.5% PF addition suggested that the poor mechanical properties of the biocomposites were likely due to poor interfacial compatibility between the matrix and fibers. Excess filler and coupling are both associated with agglomeration, which reduces compatibility with the matrix and reduces their capability to efficiently transfer stress between phases (Liu et al. 2002; Sri Aprilia et al. 2014). This confirmed our results that an increase in PF and CR lead to a decrease in tensile strength.

4.3.1.2 Young's modulus and extension at break

Young's modulus displayed nonsignificant changes with the addition of PF in both matrices (Table 4.4). PF-HDPE resulted in a decreased Young's Modulus with PF, while PF-PP appears to be unchanged by PF addition (Table 4.4). These trends were also seen in the response surface plots, which will be further discussed. The full regression model had only two significant factors, PF and plastic type (Table 4.5) (P_{PF}=0.01, $P_{plastic}$= 0.02, α=0.05). Therefore, quadratic effects were removed from the model, but this resulted in a $P_{plastic}$ of 0.07 and only one significant factor, PF (P_{PF}= 0.003)(Table 4.5). Although PF was the only significant factor of the reduced model, the linear effects of CR and plastic and all interactions were included in the model because their effects resulted in an R^2(adj) value 10.5% higher compared to a model with only PF. The

proposed model has an R^2(adj) value of 32.73%. The surface plots reflect the reduced model (Figure 4.11).

Table 4.4: Effect of peach flour (PF) loading on Young's Modulus and Extension at Break of high-density polyethylene (PE) and polypropylene (PP) composites with 5% compatibilizer resin. Different letters within a group indicate significant differences.

Formulation		**Young's Modulus (MPa)**		**Extension at Break (mm)**	
Polyolefin	**PF %wt. db**	**Average**	**Standard Deviation**	**Average**	**Standard Deviation**
PP	Control	1349.1 ^{A}	419.6	2.4 ^{A}	0.9
	2.5	1498.5 ^{A}	184.1	1.9^{AB}	0.2
	5.0	1180.8 ^{A}	183.5	1.4^{B}	0.3
	10.0	1408.8 ^{A}	207.1	1.6 ^{B}	0.3
PE	Control	1403.1 ^{A}	343.8	15.5 ^{A}	10.3
	2.5	1180.3 ^{A}	326.0	8.6 ^{AB}	3.5
	5.0	836.0 ^{A}	207.2	8.7 ^{AB}	7.5
	10.0	1092.8 ^{A}	368.4	4.1 ^{AB}	2.5

Table 4.5: Estimated variance analysis for the Young's modulus of peach flour - polyolefin biocomposites (α=0.05)

Source	**PValue**	
	Full	**Reduced**
PF	0.00514	0.00340
Plastic	0.02381	0.06927
CR	0.27353	0.11865
PF*CR	0.14745	0.12659
Plastic*CR	0.75573	0.26975
Plastic*PF	0.98072	0.57905
CR*CR	0.93268	-
PF*PF	0.75320	-
CR*CR*Plastic	0.16295	-
PF*PF*Plastic	0.98802	-

a.

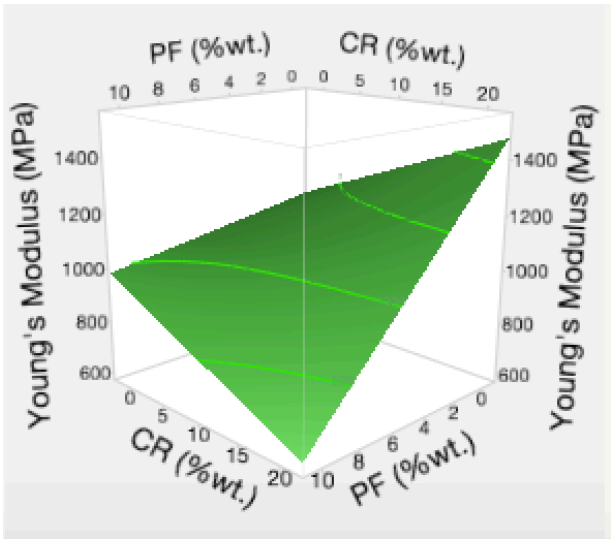

b.

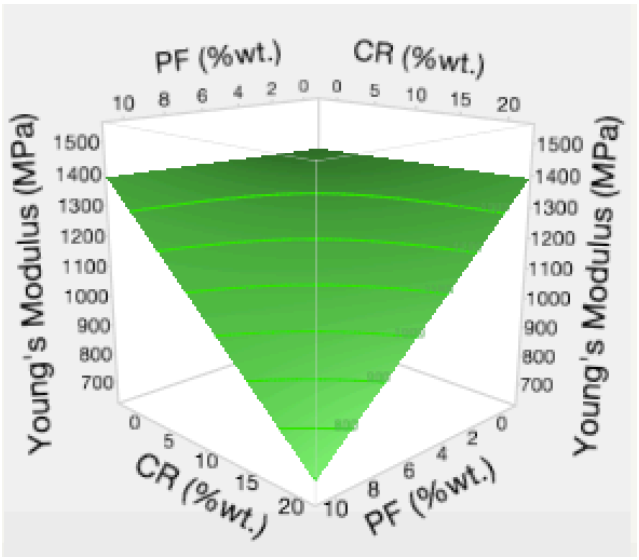

Figure 4.11: Response surface plots for the Young's Modulus of (a) high-density polyethylene and (b) polypropylene peach flour -filled biocomposites

Aforementioned, the Tukey test resulted in nonsignificant changes in Young's Modulus with PF addition for both matrices, but the response surface plots displayed noticeable trends due to factor effects (Table 4.4, Figure 4.11). Both HDPE and PP response surface plots displayed a decrease in Young's Modulus from the combined effect of PF and CR addition (Figure 4.11). The decrease in Young's Modulus was similar to results reported in the literature (Puglia et al. 2008). Authors have attributed decreases in mechanical properties to a migration of excess coupling agent around the

fibers, causing agglomeration and self-entanglement rather than interaction with the polymer matrix (Mohanty et al. 2006). High fiber concentration has also led to increased agglomeration of fiber, which reduced compatibility of filler in the matrix (Sri Aprilia et al. 2014). Not to mention the foreseen incompatibility between hydrophilic lignocellulosic fibers and hydrophobic polyolefin matrices, which has been known to challenge mechanical property enhancement in biocomposite preparation (Drzal et al. 2001). Plant fibers are hydrophilic because of the attraction between hydroxyl groups of both the fiber's structure and water molecules (Kalia et al. 2013). Polyolefins contain a carbon backbone, which is very hydrophobic and insoluble in water (Hagiopol and Johnston 2011).

Furthermore, PF-HDPE displayed obvious singular effects from PF and CR, while PP appeared to be unchanged by singular effects of PF and CR addition (Figure 4.11). The HDPE response surface plot suggested that PF would decrease Young's Modulus, which means material rigidity decreased. This decrease may be due to the rigid PF particles disrupting the matrix causing the material to become more brittle. Meanwhile, the HDPE response surface plot suggests CR could increase Young's Modulus, which would increase rigidity. This would be due to the maleic anhydride compatibilizer, which forms strong bonds with the polymer matrix and could reinforce the matrix (Jayasuriya 2017).

CR did not affect PF-PP's Young's Modulus likely due to weak interactions. Incompatibility between the PP matrix and CR was mentioned in Section 4.3.1.1 and seen in Figures 4.9 and 4.10. Since the CR was MAH-g-HDPE, the difference in polyolefins

between the CR and matrix (PP) may have negatively influenced the bonding capability between phases and led to the weak interactions.

The collected data for extension at break was highly skewed, so the data was transformed and the data was analyzed as log base-2 of the extension at break for a meaningful interpretation. All linear effects were significant in the full regression model, whereas quadratic effects were not (Table 4.6) (α=0.05). After the removal of quadratic effects, linear and interactive effects became significant and were all included in the reduced model (P<0.05, α=0.05). The proposed model had an R^2(adj) of 93.6%. The response surface plots reflect the reduced model (Figure 4.12).

Table 4.6: Estimated variance analysis for the extension at break of peach flour-polyolefin biocomposites (α=0.05)

Source	P-value	
	Full	Reduced
Plastic	0.00000	0.00000
CR	0.00001	0.00000
PF	0.00037	0.00005
Plastic*CR	0.08242	0.01817
Plastic*PF	0.00033	0.00011
PF*CR	0.04394	0.00271
PF*PF	0.90411	-
CR*CR	0.14655	-
PF*PF*Plastic	0.62356	-
CR*CR*Plastic	0.93465	-

Extension at break decreased significantly with PF addition in both matrices (Table 4.4). Both matrices resulted in a response surface model with a clear decrease in extension with PF and CR (Figure 4.12). Fiber loading was anticipated to decrease extension because fiber particles have been found to act as an interfacial discontinuity in the form of aggregates, which restrains deformation (Hidalgo-Salazar and Salinas 2019). This result has been seen in several other biocomposites, such as rice husk-PP, green

coconut-thermo plastic starch, and seaweed-HDPE composites (Albano et al. 2005; Lomelí Ramírez et al. 2011; Hidalgo-Salazar and Salinas 2019).

CR decreased extension due to the enhanced interfacial adhesion, which led to lower polymer chain mobility (Figure 4.12) (Chun et al. 2012). Even small amounts of hydrogen bonding between CR and PF can have a negative effect on chain mobility as chains can no longer slide past each other (Shakeri and Hashemi 2004; Irigoyen et al. 2019). Similar behavior has been reported in a taro powder-recycled HDPE-ethylene vinyl acetate composite made with a variety of coupling agents such as methyl methacrylate, PE-g-MAH and caprolactam-MAH (Hamim et al. 2017). All coupling agents act as reinforcement resulting in a brittle composite and reduced elongation (Ndlovu et al. 2013).

a. 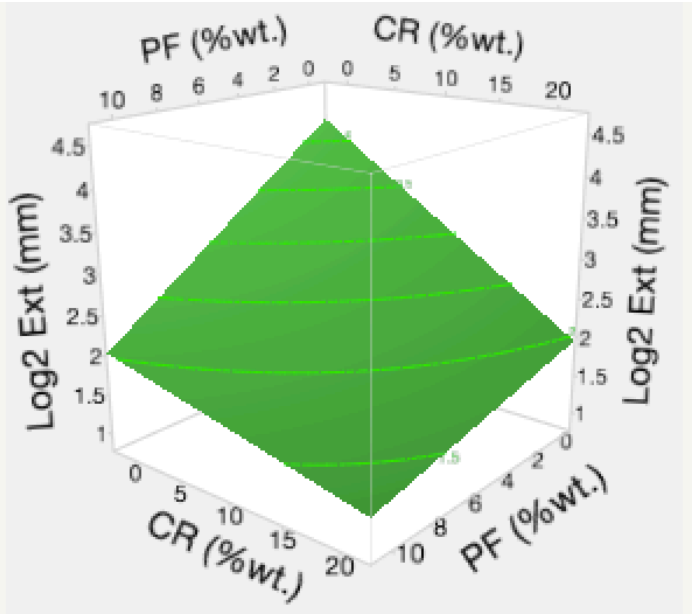

b.

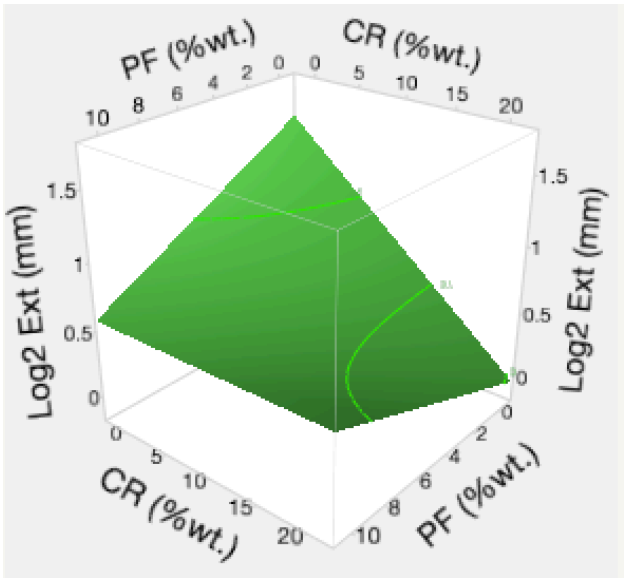

Figure 4.12: Response surface plots for the Extension at Break of (a) high-density polyethylene and (b) polypropylene peach flour composites

4.3.2 Thermal analysis

4.3.2.1 Thermogravimetric analysis

The thermal stability of the PF-polyolefin composites was determined using thermogravimetric analysis (TGA). Understanding the thermal degradation of the composite is important because polymer processing temperatures are close to the degradation temperature of natural fibers. Generally, pure PP and HDPE melt at 160°C and 120-180°C, respectively, and natural fibers begin to degrade around 200°C. Additionally, the complexity of the system may alter both the polymers and fibers' degradation profile, which is essential knowledge for the composite's final application. The degradation profile provides insight on appropriate processing temperatures, which is fundamental in polymer processing because excessive temperature-time processing conditions can oxidize and degrade resin with the probability of negatively impacting physical and mechanical properties (Selke and Culter 2016).

The TGA thermograms of the PF-PP composites were not expected. All PF-PP composite T_d values were at least 20°C higher than the control and all samples displayed an overall shift in thermal stability (Table 4.7) (Figure 4.13). The biocomposites' onset degradation temperature was ~254°C, which represented the onset of degradation for cellulose (Crews et al. 2016). The higher fiber formulation, 10% PF in PP, displayed more rapid weight loss and additional derivative weight peaks at 271°C and 340°C. These peaks, which were also seen in the PF thermogram, reflected the degradation of cellulose and lignin, respectively (Figure 4.2). The tallest biocomposite derivative weight peaks were at ~434°C, while the control's peak was at 406°C (Figure 4.13). The derivative weight peak decreased by 0.5%/°C when PF increased from 2.5 to 10%wt.

Previous research exploring coconut shell powder-PLA and rice husk-PP biocomposites reported an increase in biocomposite thermal stability in the presence of natural fiber (Chun et al. 2012; Hidalgo-Salazar and Salinas 2019). This increase was attributed to the char formation during fiber pyrolysis, as char may act as a protective barrier from thermal decomposition (Perinović et al. 2010; Chun et al. 2012). Char formation is represented in the residue value (Table 4.7). The increase in residue is due to the chemical structure of lignin, which contains a phenylpropanoid unit with aromatic phenyl groups that contribute to lignin's ability to char and slow thermal degradation (Ghozali et al. 2017). The derivative weight peaks decreased with PF loading likely because the higher lignin content contributed to slower degradation and weight loss. This shift in thermal stability was unlikely to be due to CR addition. Previous research has suggested that coupling agent addition can accelerate degradation by destroying polymer crystal structures therefore promoting thermal degradation (Zhang et al. 2017).

Table 4.7: Effect of peach flour loading on the degradation temperatures (T_d) and %residues on peach flour-polyolefin composites through thermogravimetric analysis

Formulation		T_d (°C)	Derivative Weight Peak (%/°C)	Residue (%)
Polyolefin	**PF %wt. db**			
PP	Control	334.7	406.8	<0.1
	2.5	369.1	435.4	0.8
	5.0	363.4	434.1	1.9
	10.0	367.7	433.6	4.0
PE	Control	413.1	455.12	0.7
	2.5	413.5	457.11	1.4
	5.0	420.9	458.45	1.8
	10.0	414.2	456.38	3.0

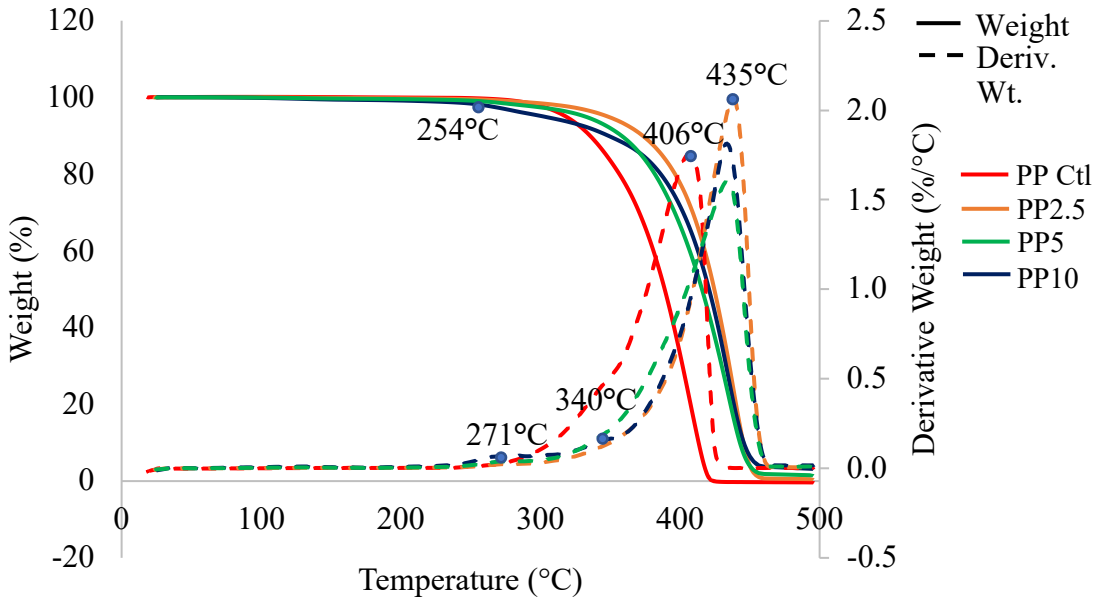

Figure 4.13: Thermogravimetric analysis thermogram for peach flour -polypropylene composites with increasing peach flour loading and 5% compatibilizer resin

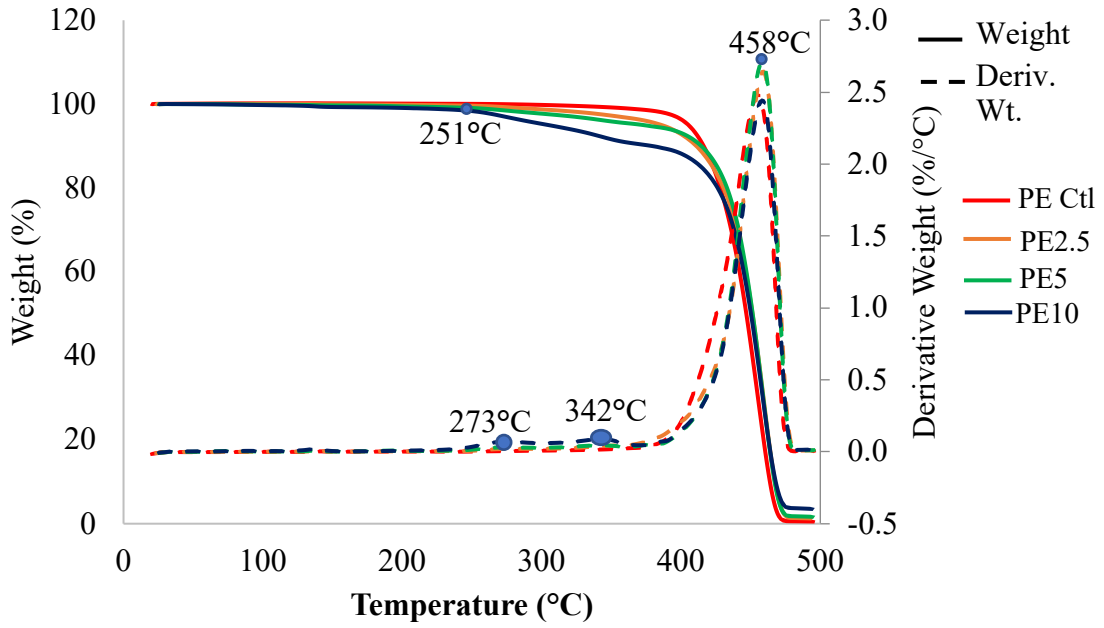

Figure 4.14: Thermogravimetric analysis thermogram for peach flour high-density polyethylene composites with increasing peach flour loading and 5% compatibilizer resin

On the other hand, the PF-PE composites displayed no shift in thermal stability compared to the PE control (Table 4.7, Figure 4.13). PE with 5% PF resulted in a T_d ~7°C higher than the remaining HDPE samples, but its thermogram displayed no shift in thermal stability (Table 4.7, Figure 4.13). All derivative weight peaks were ~456°C with a derivative weight of ~2%/°C. The HDPE biocomposites did display onset degradation values of 251°C, as seen in the PP formulations, representative of the onset of cellulose degradation (Figure 4.14 and 4.13). The formulations with higher PF loading (HDPE with 5 and 10% PF) again displayed rapid weight loss and additional derivative weight peaks at 273°C and 342°C reflecting the degradation of cellulose and lignin, respectively.

PF-HDPE biocomposites displayed no shift in thermal stability likely because of HDPE's naturally high degradation temperature of ~460°C, which did not display any enhancement from the thermal stability of lignin. Another possible explanation is that there was no interaction between filler and matrix and the filler did not disturb the

degradation process (Perinović et al. 2010; Hidalgo-Salazar and Salinas 2019). Interactions should be confirmed through spectroscopic analysis.

The biocomposites did not display any decrease in thermal stability, which led us to conclude that PF-polyolefin biocomposites are capable of thermal processing. HDPE and PP can be processed below 200°C, which is the recommended processing temperature to preserve the mechanical properties natural fibers (Velde and Kiekens 2003; John and Anandjiwala 2009).

4.3.2.2 Differential scanning calorimetry

DSC measures the heat flow through the sample compared to a reference to identify phase changes. The data collected for this study was: melting temperature (T_m), crystallization temperature (T_c), crystallization enthalpy, and percent crystallinity (Table 4.8). The crystallinity of 2.5% PF-PP decreased from 75.5% to 42.6% and continued to decrease with PF loading (Table 4.8). Along with crystallinity, the enthalpy of crystallization decreased across all biocomposite formulations, which means there was a reduction in the energy required to crystallize the matrix. Polymer chain movement may have been restricted by the addition of fibers, which may act as an obstacle for crystal formation and decrease crystallization enthalpy (Lee and Wang 2006; Perinović et al. 2010). Crystallinity influences the optical, mechanical, thermal, and chemical properties of the polymers. A reduction in crystallinity leads to a reduction in density, tensile strength, melting temperature, and opacity, while increasing elongation, toughness, and impact strength (Selke and Culter 2016). The desired polymer crystallinity varies with the polymer application. For example, highly crystalline polymers can be made into rigid containers, while low crystallinity polymers can be made into plastic bags. PF-HDPE

biocomposite at 2.5% PF displayed a 2.7% increase in crystallinity compared to pure virgin HDPE (Table 4.8). This increase may be attributed to fibers increasing the number of nucleating sites to enhance crystallinity (Avérous and Le Digabel 2006). The imperfections and defects of fiber surfaces may favor and initiate the growth of crystals, as seen in wood flour-PLA biocomposites (Mathew et al. 2006). The decreased T_c values for biocomposites was another indication of the nucleating ability of fillers (Table 4.8) (Wang et al. 2018). Beyond 2.5% PF the HDPE biocomposite crystallinity decreased 3% lower than the pure virgin HDPE and continued to decrease with PF loading. PF had no influence on T_m indicating that the filler does not disturb the melting process (Perinović et al. 2010). Similar results have been reported in a silica-HDPE composite (Jeziórska et al. 2014). The HDPE glass transition temperature (T_g) could not be observed as pure HDPE has a T_g value of -110°C (Wang et al. 2007). PP did not display its expected T_g of -10°C, therefore the provided PP was crystalline and remains crystalline during the glass transition.

Table 4.8: Effect of peach flour loading on differential scanning calorimetry values for peach flour-polyolefin composites with increasing peach flour loading and 5% compatibilizer resin

Formulation		**T_c (°C)**	**Enthalpy of crystallization (j/g)**	**T_m (°C)**	**%Crystallinity**
Polyolefin	**PF %wt. db**				
PP	Control	123.07	153.30	165.85	75.5%
	2.5	117.59	104.90	162.09	42.6%
	5.0	116.11	91.80	161.17	38.7%
	10.0	116.24	94.66	162.33	39.4%
PE	Control	118.66	210.70	133.87	77.0%
	2.5	118.58	196.50	134.35	79.1%
	5.0	119.83	186.00	133.44	74.7%
	10.0	118.25	148.37	134.58	62.4%

4.3.3 Water absorption

Water absorption is the capacity of a polymer to absorb moisture from its environment. In general, water uptake in a composite will increase with fiber loading, hydrophilicity, and composite porosity (Sultana and Khan 2013). The percent increase in weight due to water absorption is presented in Table 4.9. The data displayed an increase in water absorption with PF loading (Table 4.9). The collected data was highly skewed, so the data was transformed and the data was analyzed as log of the percent absorption for a meaningful interpretation. Quadratic and interactive effects were all nonsignificant as illustrated by a p-value higher than 0.05, therefore they were removed from the model (Table 4.10). Although the P_{CR} was greater than 0.05 in the reduced model, it still increased the R^2(adj) value by 1.2% compared to a model with only PF and plastic type. Therefore, CR was kept in the model. The reduced model had an R^2(adj) of 65.52%, which was reflected in the response surface plot (Figure 4.15).

Table 4.9: Water absorption for peach flour-polyolefin composites with increasing peach flour loading and 5% compatibilizer resin

Formulation		%Increase
Polyolefin	%PF	
PP	Control	0.08%
	2.5	0.08%
	5	0.19%
	10	0.30%
PE	Control	0.06%
	2.5	0.17%
	5	0.49%
	10	0.94%

Table 4.10: Estimated variance analysis for the %absorbance of peach flour -polyolefin biocomposites (α=0.05)

Source	PValue	
	Full	Reduced
PF	0.00000	0.00000
Plastic	0.05174	0.02216
PF*CR	0.10537	-
Plastic*PF*PF	0.25857	-
CR	0.37249	0.16459
PF*PF	0.38219	-
Plastic*CR	0.42933	-
Plastic*PF	0.50255	-
Plastic*PF*CR	0.71858	-
Plastic*CR*CR	0.88621	-
CR*CR	0.97599	-

a.

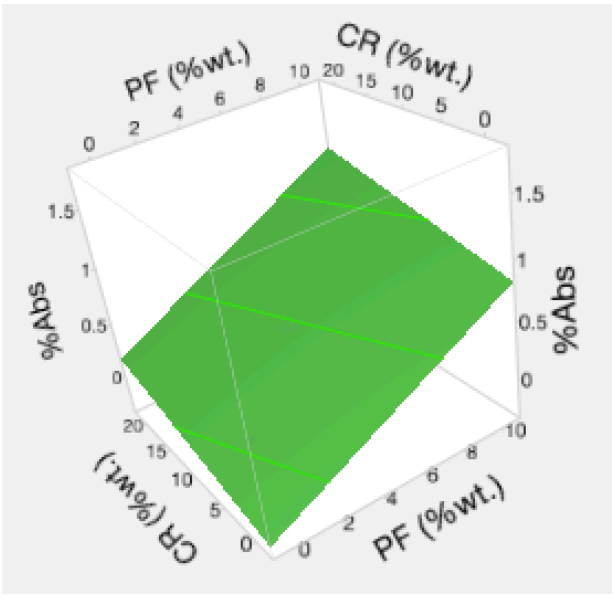

b.

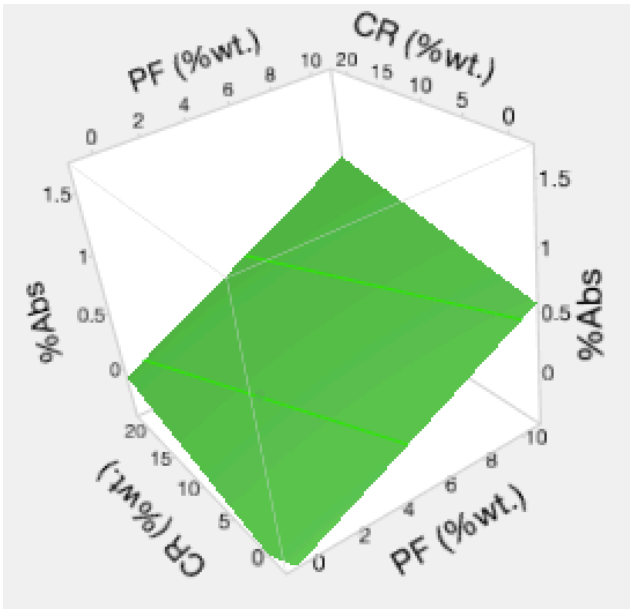

Figure 4.15: Response surface plots for water absorption of (a) high-density polyethylene and (b) polypropylene peach flour -filled biocomposites

As previously reported, water absorption significantly increased with fiber loading ($P<0.1$, $\alpha=0.05$) (Figure 4.15). There was not enough evidence to prove CR had an effect on water absorption properties ($P>0.05$, $\alpha=0.05$). Water absorption increased with fiber content likely because of the increased number of hydroxyl groups capable of forming hydrogen bonds with water. Additionally, high fiber loading leads to poor interfacial bonding, which increases the number of micro-voids, causing increased water absorption (Yang et al. 2006). However, the highest water absorption demonstrated was 0.90% for the 10%. PF-PE formulation, which was relatively low compared to a 10% rice husk-thermoplastic starch composite, which had a reported absorption of ~7% (Table 4.9). This result was similar to the behavior of a walnut shell-thermoplastic composite (Singh et al. 2019). This relatively low water absorption was likely due the higher lignin content and lower content of highly hydrophobic materials, cellulose and hemicellulose.

CONCLUSION

The objectives of this research were (1) to develop maleic anhydride compatibilized PF biocomposites with PP and HDPE matrices and (2) to evaluate the biocomposites' mechanical, thermal, and water absorption properties. It was hypothesized that maleic anhydride compatibilized PF could serve as a viable filler in a polyolefin matrix because peach stones offer a high lignin content for interaction between the compatibilizer and polymer matrix.

A low PF loading (<2.5%) and 5% CR loading produced HDPE and PP biocomposites with comparable tensile strength, young's modulus, and extension break properties to their virgin, pure polyolefin controls. Filler loadings of 5% and greater generally demonstrated a decrease in mechanical properties because of the incompatibility between hydrophilic fibers and hydrophobic polymers. The incompatibility ultimately lead to agglomeration, which reduced the capability of efficient stress transfer between phases. Since all mechanical properties either remained unchanged or significantly decreased with fiber loading, the results suggested that PF possesses poor mechanical properties unsuitable for biocomposite mechanical strength enhancement.

PF addition caused a shift in the thermal degradation of PP biocomposites, which was attributed to lignin's complex structure which imparts high char capability, as char may act as a protective barrier against decomposition. The HDPE biocomposites displayed no change in degradation temperature or melting temperature indicating that the filler did not interfere with the degradation or melting process. The crystallinity of

both PP and HDPE decreased with PF loading likely because fillers restricted polymer movement and acted as an obstacle for crystal formation.

Water absorption increased with fiber loading because of the increased number of hydroxyl groups capable of bonding with water. However, the relatively high lignin content of PF imparts higher water absorption resistance compared to high cellulose content fibers.

It was concluded that a PF-polyolefin biocomposite with 2.5% filler loading and 5% CR could produce a plastic material comparable to a neat polyolefin matrix. This would reduce petroleum consumption and could divert approximately 1,302 tons of peach waste from the landfill. Potential applications for this material include non-load bearing commodities such as packaging and automotive parts and consumer goods.

Future research should explore physical and mechanical properties of PF to identify its strengths and determine its best application. Additionally, future research should examine the morphological structure of PF-polyolefin biocomposites using spectroscopy and microscopy to confirm bonding capability and identify opportunities for improvement.

BIBLIOGRAPHY

Aghdam EF, Scheutz C, Kjeldsen P (2019) Impact of meteorological parameters on extracted landfill gas composition and flow. Waste Manag 87:905–914.

Albano C, Karam A, Domínguez N, Sánchez Y, González J, Aguirre O, Cataño L (2005) Thermal, mechanical, morphological, thermogravimetric, rheological and toxicological behavior of HDPE/seaweed residues composites. Compos Struct 71:282–288.

Alemdar A, Sain M (2008) Biocomposites from wheat straw nanofibers: Morphology, thermal and mechanical properties. Compos Sci Technol 68:557–565.

Altınkaynak A (2010) Three dimensional finite element simulation of polymer melting and flow in a single-screw extruder: Optimization of screw channel geometry. Michigan Technological University.

Amir N, Abidin KAZ, Shiri FBM (2017) Effects of fibre configuration on mechanical properties of banana fibre/PP/MAPP natural fibre reinforced polymer composite. Procedia Eng 184:573–580.

Annisa AN, Widayat W (2018) A review of bio-lubricant production from vegetable oils using esterification transesterification process. MATEC Web Conf 156:1–7.

AOAC (2000) Official Methods of Analysis Official Method 991.36, 17th edn. Gaithersburg, MD.

Argun H, Dao S (2017) Bio-hydrogen production from waste peach pulp by dark fermentation: Effect of inoculum addition. Int J Hydrogen Energy 42:2569–2574.

Arvelakis S, Gehrmann H, Beckmann M, Koukios EG (2005) Preliminary results on the ash behavior of peach stones during fluidized bed gasification: evaluation of fractionation and leaching as pre-treatments. Biomass and Bioenergy 28:331–338.

Avérous L, Le Digabel F (2006) Properties of biocomposites based on lignocellulosic fillers. Carbohydr Polym 66:480–493.

Awotedu OL, Ogunbamowo PO, Awotedu BF, Ariwoola OS (2020) Comparative nutritional composition of selected medicinal fruit seeds. 29:298–310.

Ayala-Zavala JF, Vega-Vega V, Rosas-Domínguez C, Palafox-Carlos H, Villa-Rodriguez JA, Siddiqui MW, Dávila-Aviña JE, González-Aguilar GA (2011) Agro-industrial potential of exotic fruit byproducts as a source of food additives. Food Res Int 44:1866–1874.

Ayrilmis N, Jarusombuti S, Fueangvivat V, Bauchongkol P, White RH (2011) Coir fiber reinforced polypropylene composite panel for automotive interior applications.

Fibers Polym 12:919–926.

Badia JD, Strömberg E, Karlsson S, Ribes-Greus A (2012) Material valorisation of amorphous polylactide. Influence of thermo-mechanical degradation on the morphology, segmental dynamics, thermal and mechanical performance. Polym Degrad Stab 97:670–678.

Banat R (2019) Olive pomace flour as potential organic filler in composite materials : A brief review. Am J Polym Sci 9:10–15.

Bao W, O'Malley DM, Sederoff RR (1992) Wood contains a cell-wall structural protein. Proc Natl Acad Sci U S A 89:6604–6608.

Barboza LGA, Dick Vethaak A, Lavorante BRBO, Lundebye AK, Guilhermino L (2018) Marine microplastic debris: An emerging issue for food security, food safety and human health. Mar Pollut Bull 133:336–348.

Barlaz MA, Chanton JP, Green RB (2009) Controls on landfill gas collection efficiency: Instantaneous and lifetime performance. J Air Waste Manag Assoc 59:1399–1404.

Barletta M, Pizzi E, Puopolo M, Vesco S (2017) Design and manufacture of degradable polymers: Biocomposites of micro-lamellar talc and poly(lactic acid). Mater Chem Phys 196:62–74.

Bassi D, Mignani I, Spinardi A, Tura D (2015) Peach (Prunus persica (L.) Batsch). In: Simmonds M, Preedy V (eds) Nutritional Composition of Fruit Cultivars. Elsevier Inc., Waltham, MA, pp 535–571.

Beigbeder J, Soccalingame L, Perrin D, Bénézet JC, Bergeret A (2019) How to manage biocomposites wastes end of life? A life cycle assessment approach (LCA) focused on polypropylene (PP)/wood flour and polylactic acid (PLA)/flax fibres biocomposites. Waste Manag 83:184–193.

Beyler CL, Hirschler MM (2002) Thermal Decomposition of Polymers. In: SFPE Handbook of Fire Protection Engineering. National Fire Protection Association, pp 111–131.

Bledzki AK, Franciszczak P, Osman Z, Elbadawi M (2015) Polypropylene biocomposites reinforced with softwood, abaca, jute, and kenaf fiber. Ind Crop Prod J 70:91–99.

Bledzki AK, Mamun AA, Volk J (2010) Barley husk and coconut shell reinforced polypropylene composites: The effect of fibre physical, chemical and surface properties. Compos Sci Technol 70:840–846.

Bolarinwa IF, Orfila C, Morgan MRA (2014) Amygdalin content of seeds, kernels and food products commercially- available in the UK. Food Chem 152:133–139.

Bos HL, Müssig J, van den Oever MJA (2006) Mechanical properties of short-flax-fibre

reinforced compounds. Compos Part A Appl Sci Manuf 37:1591–1604.

Bourmaud A, Baley C (2007) Investigations on the recycling of hemp and sisal fibre reinforced polypropylene composites. Polym Degrad Stab 92:1034–1045.

Bradford A, Sunby J, Truelove A, Andre A (2019) Composting in America: A path to eliminate waste, revitalize soil and tackle global warming. Washington, DC.

Calabia BP, Ninomiya F, Yagi H, Oishi A, Taguchi K, Kunioka M, Funabashi M (2013) Biodegradable poly(butylene succinate) composites reinforced by cotton fiber with silane coupling agent. Polymers (Basel) 5:128–141.

Chaitanya S, Singh I, Song J Il (2019) Recyclability analysis of PLA/Sisal fiber biocomposites. Compos Part B Eng 173:1–9.

Chun KS, Husseinsyah S, Osman H (2012) Mechanical and thermal properties of coconut shell powder filled polylactic acid biocomposites: Effects of the filler content and silane coupling agent. J Polym Res 19:1–8.

Cornell DD (2007) Biopolymers in the existing postconsumer plastics recycling stream. J Polym Environ 15:295–299.

Correa CA, Razzino CA, Hage E (2007) Role of maleated coupling agents on the interface adhesion of polypropylene-wood composites. J Thermoplast Compos Mater 20:323–339.

Crespy D, Bozonnet M, Meier M (2008) 100 Years of Bakelite, the material of a 1000 uses. Angew Chemie - Int Ed 47:3322–3328.

Crews K, Huntley C, Cooley D, Phillips B, Curry M (2016) Influence of cellulose on the mechanical and thermal stability of ABS plastic composites. Int J Polym Sci 2016:1–10.

Dardick C, Callahan AM (2014) Evolution of the fruit endocarp: molecular mechanisms underlying adaptations in seed protection and dispersal strategies. Front Plant Sci 5:1–10.

Dauvergne P (2018) Why is the global governance of plastic failing the oceans? Glob Environ Chang 51:22–31.

DeArmitt C, Rothon R (2017) Applied Plastics Engineering Handbook: Plastic Additives. In: Kutz M (ed) Applied Plastics Engineering Handbook, 2nd edn. Cambridge, MA, pp 489–500.

Déjardin A, Laurans F, Arnaud D, Breton C, Pilate G, Leplé JC (2010) Wood formation in Angiosperms. Comptes Rendus - Biol 333:325–334.

Dentener FJ, Easterling DR, Uk RA, Uk RA, Cooper O, Canada F, Uk JK, Uk EK,

Germany SK, Uk CM, Morice C (2013) IPCC Climate Change 2013: The Physical Science Basis. Chapter 2: Observations: Atmosphere and Surface. Clim Chang 2013 Phys Sci Basis Work Gr I Contrib to Fifth Assess Rep Intergov Panel Clim Chang 9781107057:159–254.

Dhakal HN, Zhang ZY, Richardson MOW (2007) Effect of water absorption on the mechanical properties of hemp fibre reinforced unsaturated polyester composites. Compos Sci Technol 67:1674–1683.

Dinh Vu N, Thi Tran H, Duy Nguyen T (2018) Characterization of polypropylene green composites reinforced by cellulose fibers extracted from rice straw. Int J Polym Sci 2018:1–10.

Dixon R, Paiva N (1995) Stress-induced phenylpropanoid metabolism. Am Soc Plant Physiol 7:1085–1097.

Djafari Petroudy SR (2017) Physical and mechanical properties of natural fibers. In: Fan M, Fu F (eds) Advanced High Strength Natural Fibre Composites in Construction. Woodhead Publishing, pp 59–83.

Drobny JG (2014) Processing Methods Applicable to Thermoplastic Elastomers. In: Handbook of Thermoplastic Elastomers. William Andrew Publishing, pp 33–173.

Drzal LT, Mohanty AK, Misra M (2001) Bio-composite materials as alternatives to petroleum-based composites for automotive applications. Compos Mater Struct Cent 40:1–8.

Eagle L, Hamann M, Low DR (2016) The role of social marketing, marine turtles and sustainable tourism in reducing plastic pollution. Mar Pollut Bull 107:324–332.

Ehrlich PR, Harte J (2015) Food security requires a new revolution. Int J Environ Stud 72:908–920.

El-Sabbagh A (2014) Effect of coupling agent on natural fibre in natural fibre/polypropylene composites on mechanical and thermal behaviour. Compos Part B Eng 57:126–135.

Endres H-J, Hausmann K, Helmke P (2006) Untersuchungen des einflusses unterschiedlicher haftvermittler und haftvermittlerge- halte auf PP-holzmehl-compoundsle (in German). KGK Kautschuk Gummi Kunststoffe 59:399.

EPA (2020a) Benefits of Landfill Gas Energy Projects. In: Landfill Methane Outreach Progr. https://www.epa.gov/lmop/accomplishments-landfill-methane-outreach-program. Accessed 2 Jun 2020.

EPA (2011) Available and emerging technologies for reducing greenhouse gas emissions from municipal solid waste landfills. United States Environ Prot Agency Off Air Radiation 6–7.

EPA (2020b) Project and Landfill Data by State. In: Landfill Methane Outreach Progr. https://www.epa.gov/lmop/project-and-landfill-data-state. Accessed 2 Jun 2020.

EPA (2020c) National Overview: Facts and Figures on Materials, Wastes and Recycling. In: Facts Fig. about Mater. Waste Recycl. https://www.epa.gov/facts-and-figures-about-materials-waste-and-recycling/guide-facts-and-figures-report-about-materials. Accessed 2 Jun 2020.

Essabir H, Bensalah MO, Bouhfid R, Qaiss A (2014) Fabrication and characterization of apricot shells particles reinforced high density polyethylene based bio-composites: Mechanical and thermal properties. J Biobased Mater Bioenergy 8:344–351.

Essabir H, Bensalah MO, Rodrigue D, Bouhfid R, Qaiss AEK (2016) Biocomposites based on Argan nut shell and a polymer matrix: Effect of filler content and coupling agent. Carbohydr Polym 143:70–83.

Eteläaho P, Nevalainen K, Suihkonen R, Vuorinen J, Hanhi K, Järvelä P (2009) Effects of direct melt compounding and masterbatch dilution on the structure and properties of nanoclay-filled polyolefins. Polym Eng Sci 49:1438–1446.

Fan J, Nassiopoulos E, Brighton J, Larminat A De, Njuguna J (2011) New Structural Bio Composites for Car Applications. Soc Plast Eng - Eurotec 2011 1–5.

FAO (2011) Global Food Loss and Food Waste - Extent, causes and prevention. Food and Agriculture Organization of the United Nations, Rome, Italy.

Faruk O, Bledzki AK, Fink H-P, Sain M (2012) Biocomposites reinforced with natural fibers: 2000–2010. Prog Polym Sci 37:1552–1596.

Fresh Del Monte (2014) Del Monte Sustainability Report: Waste Management. Walnut Creek, CA.

Fu SY, Lauke B (1997) The fibre pull-out energy of misaligned short fibre composites. J Mater Sci 32:1985–1993.

Gall SC, Thompson RC (2015) The impact of debris on marine life. Mar Pollut Bull 92:170–179.

Garcia-Jaldon C, Dupeyre D, Vignon MR (1998) Fibres from semi-retted hemp bundles by steam explosion treatment. Biomass and Bioenergy 14:251–260.

Gassan J, Bledzki AK (1997) The influence of fiber-surface treatment on the mechanical properties of jute-polypropylene composites. Compos Part A Appl Sci Manuf 28:1001–1005.

George M, Mussone PG, Bressler DC (2014) Surface and thermal characterization of natural fibres treated with enzymes. Ind Crops Prod 53:365–373.

Ghasemi A, Abbas EPH, Farhang L, Bagheri1 R (2018) Polypropylene/plant-based fiber biocomposites and bionanocomposites. In: PM V, Poletto M (eds) Polypropylene-Based Biocomposites and Bionanocomposites. Scrivener Pubslishing, Beverly, MA, pp 247–286.

Ghozali M, Triwulandari E, Haryono A, Yuanita E (2017) Effect of lignin on morphology, biodegradability, mechanical and thermal properties of low linear density polyethylene/lignin biocomposites. IOP Conf Ser Mater Sci Eng 223:1–13.

Gopanna A, Rajan KP, Thomas SP, Chavali M (2019) Polyethylene and polypropylene matrix composites for biomedical applications. In: Grumezescu V, Grumezescu A (eds) Materials for Biomedical Engineering, 1st edn. Elsevier, pp 175–216.

Gradziel T, McCaa J (2008) Processing Peach Cultivar Development T.M. In: Layne D, Bassi D (eds) The Peach: Botany, Production and Uses. CAB International, Cambridge, MA, pp 175–192.

Graupner N (2008) Application of lignin as natural adhesion promoter in cotton fibre-reinforced poly(lactic acid) (PLA) composites. J Mater Sci 43:5222–5229.

Graupner N, Müssig J (2017) Cellulose fiber-reinforced PLA versus PP. Int J Polym Sci 2017:1–10.

Graupner N, Ziegmann G, Wilde F, Beckmann F, Müssig J (2016) Procedural influences on compression and injection moulded cellulose fibre-reinforced polylactide (PLA) composites: Influence of fibre loading, fibre length, fibre orientation and voids. Compos Part A Appl Sci Manuf 81:158–171.

Gu R, Sain M, Kokta B V., Law KN (2015) The role of nanoclay formations and wood fiber levels on central composite designed polyethylene composites. J Compos Mater 49:1127–1139.

Gurunathan T, Mohanty S, Nayak SK (2015) A review of the recent developments in biocomposites based on natural fibres and their application perspectives. Compos Part A Appl Sci Manuf 77:1–25.

Hagiopol C, Johnston JW (2011) From Wood to Paper A General View of the Papermaking Process. In: Chemistry of Modern Papermaking. CRC Press, pp 5–50.

Hamim FAR, Ghani SA, Zainuddin F (2017) Influences of the coupling agent and various compatibilisers on properties of recycled high density polyethylene/ethylene vinyl acetate/taro powder (Colocasia esculenta) biocomposites. J Phys Sci 28:71–84.

Han SO, Lee SM, Park WH, Cho D (2006) Mechanical and thermal properties of waste silk fiber-reinforced poly(butylene succinate) biocomposites. J Appl Polym Sci 100:4972–4980.

Hermawan B, Nikmatin S, Sudaryanto, Alatas H, Sukaryo SG (2017) Effect of oil palm

empty fruit bunches fibers reinforced polymer recycled. IOP Conf Ser Mater Sci Eng 223:1–9.

Herrera Franco P, Valadez-González A (2005) Natural Fibers, Biopolymers, and Biocomposites. In: Mohanty AK, Misra M, Drzal LT (eds) Natural Fibers, Biopolymers, and Biocomposites. Taylor and Francis, Boca Raton, FL, pp 177–230.

Hidalgo-Salazar MA, Salinas E (2019) Mechanical, thermal, viscoelastic performance and product application of PP- rice husk Colombian biocomposites. Compos Part B Eng 176:107135.

Hill CA., Khalil HPSA, Hale MD (1998) A study of the potential of acetylation to improve the properties of plant fibres. Ind Crops Prod 8:53–63.

Hills D, Roberts D (1982) Conversion of Tomato, Peach and Honeydew Solid Waste into Methane Gas. Trans ASAE 25:820–826.

Huda MS, Drzal LT, Mohanty AK, Misra M (2008) Effect of fiber surface-treatments on the properties of laminated biocomposites from poly(lactic acid) (PLA) and kenaf fibers. Compos Sci Technol 68:424–432.

Irigoyen M, Matxain JM, Ruipérez F (2019) Effect of molecular structure in the chain mobility of dichalcogenide-based polymers with self-healing capacity. Polymers (Basel) 11:1–14.

Jambeck J, Geyer R, Wilcox C, Siegler T, Narayan R, Law K (2015) Plastic waste inputs from land into the ocean. Sci. Mag. 347:768–771.

Jayasuriya CK (2017) Interfacial Bonding in Polymer–Ceramic Nanocomposites. In: Reference Module in Materials Science and Materials Engineering. Elsevier, pp 1–6.

Jeziórska R, Zielecka M, Gutarowska B, Zakowska Z (2014) High-density polyethylene composites filled with nanosilica containing immobilized nanosilver or nanocopper: Thermal, mechanical, and bactericidal properties and morphology and interphase characterization. Int J Polym Sci 2014:1–14.

Jiang L, Zhang J (2017) Biodegradable and Biobased Polymers. In: Kutz M (ed) Applied Plastics Engineering Handbook: Processing, Materials, and Applications, 2nd edn. Elesevier Inc., Cambridge, MA, pp 127–143.

John MJ, Anandjiwala RD (2008) Recent developments in chemical modification and characterization of natural fiber-reinforced composites. Polym Compos 29:187–207.

John MJ, Anandjiwala RD (2009) Chemical modification of flax reinforced polypropylene composites. Compos Part A Appl Sci Manuf 40:442–448.

Kaboorani A (2010) Effects of formulation design on thermal properties of wood/thermoplastic composites. J Compos Mater 44:2205–2215.

Kalia S, Thakur K, Celli A, Kiechel MA, Schauer CL (2013) Surface modification of plant fibers using environment friendly methods for their application in polymer composites, textile industry and antimicrobial activities: A review. J Environ Chem Eng 1:97–112.

Karpenja T, Lorentzon A, Wickholm K (2013) Sustainability aspects in waste management of biocomposites. In: 26th IAPRI symposium, June 10-13 2013. IAPRI Symposium on Packaging, Stockholm, Sweden, pp 220–232.

Kaur G, Luo L, Chen G, Wong JWC (2019) Integrated food waste and sewage treatment – A better approach than conventional food waste-sludge co-digestion for higher energy recovery via anaerobic digestion. Bioresour Technol 289:1–10.

Kaynak B, Topal H, Atimtay AT (2005) Peach and apricot stone combustion in a bubbling fluidized bed. Fuel Process Technol 86:1175–1193.

Keener TJ, Stuart RK, Brown TK (2004) Maleated coupling agents for natural fibre composites. Compos Part A Appl Sci Manuf 35:357–362.

Khalid M, Ali S, Abdullah L., Ratnam C., Thomas Choong S. (2006) Preparation of composite effect of MAPP as coupling agent on the mechanical properties of palm fiber empty fruit bunch and cellulose polypropylene biocomposites. Int J Eng Technol 3:79–84.

Kjeldahl J (1883) Neue Methode zur Bestimmung des Stickstoffs in organischen Körpern. [New Method for the Determination of Nitrogen in Organic Substances.]. Zeitschrift für Anal Chemie 22:366–383.

Klemchuk PP (1990) Degradable plastics: A critical review. Polym Degrad Stab 27:183–202.

Kuzmanović M, Delva L, Mi D, Martins CI, Cardon L, Ragaert K (2018) Development of crystalline morphology and its relationship with mechanical properties of PP/PET microfibrillar composites containing POE and POE-g-MA. Polymers (Basel) 10:291–308.

Lee SH, Oh A, Shin SH, Kim HN, Kang WW, Chung SK (2017) Amygdalin contents in peaches at different fruit development stages. Prev Nutr Food Sci 22:237–240.

Lee SH, Wang S (2006) Biodegradable polymers/bamboo fiber biocomposite with bio-based coupling agent. Compos Part A Appl Sci Manuf 37:80–91.

Lee SM (1993) Braiding. In: Lee SM (ed) Handbook of Composite Reinforcements. John Wiley & Sons, pp 24–40.

Li X, Panigrahi S, Tabil LG (2009) A study on flax fiber-reinforced polyethylene biocomposites. Appl Eng Agric 25:525–531.

Li X, Tabil LG, Panigrahi S (2007) Chemical treatments of natural fiber for use in natural fiber-reinforced composites: A review. J Polym Environ 15:25–33.

Liu R, Peng Y, Cao J, Chen Y (2014) Comparison on properties of lignocellulosic flour/polymer composites by using wood, cellulose, and lignin flours as fillers. Compos Sci Technol 103:1–7.

Liu ZH, Kwok KW, Li RKY, Choy CL (2002) Effects of coupling agent and morphology on the impact strength of high density polyethylene/CaCO composites. Polymer (Guildf) 43:2501–2506.

Lomelí Ramírez MG, Satyanarayana KG, Iwakiri S, de Muniz GB, Tanobe V, Flores-Sahagun TS (2011) Study of the properties of biocomposites. Part I. Cassava starch-green coir fibers from Brazil. Carbohydr Polym 86:1712–1722.

Manikandan Nair K., Thomas S, Groeninckx G (2001) Thermal and dynamic mechanical analysis of polystyrene composites reinforced with short sisal fibres. Compos Sci Technol 61:2519–2529.

Mansor M, Mustafa Z, Fadzullah SHSM, Omar G, Salim MA, Akop MZ (2018) Recent Advances in Polyethylene-Based Biocomposites. In: Sapuan S, Ismail H, Zainudin E (eds) Natural Fibre Reinforced Vinyl Ester and Vinyl Polymer Composites. Woodhead Publishing, pp 71–96.

Mansor M, Sapuan S, Zainudin E, Aziz N (2015) Life Cycle Assessment of Natural Fiber Polymer Composites. In: Hakeem K, Jawaid M, Alothman O Y (eds) Agricultural Biomass Based Potential Materials. Springer, pp 121–141.

Marković S, Stanković A, Lopičić Z, Lazarević S, Stojanović M, Uskoković D (2015) Application of raw peach shell particles for removal of methylene blue. J Environ Chem Eng 3:716–724.

Mathew AP, Oksman K, Sain M (2006) The effect of morphology and chemical characteristics of cellulose reinforcements on the crystallinity of polylactic acid. J Appl Polym Sci 101:300–310.

McClements J (2003) Determination of Ash Content: Dry Ashing. In: Anal. Ash Miner. https://people.umass.edu/~mcclemen/581Ash&Minerals.html#:~:text=A number of dry ashing,oC for 24 hours.

Mendu V, Harman-Ware AE, Placido A, DeBolt S, Crocker M, Huber G, Morton S, Jae J, Stork J, Mendu V (2011) Identification and thermochemical analysis of high-lignin feedstocks for biofuel and biochemical production. Biotechnol Biofuels 4:43–56.

Mishra S, Misra M, Tripathy SS, Nayak SK, Mohanty AK (2001) Graft copolymerization of acrylonitrile on chemically modified sisal fibers. Macromol Mater Eng 286:107–113.

Miwa M, Horiba N (1994) Effects of fibre length on tensile strength of carbon/glass fibre hybrid composites. J Mater Sci 29:973–977.

Mohanty S, Verma SK, Nayak SK (2006) Dynamic mechanical and thermal properties of MAPE treated jute/HDPE composites. Compos Sci Technol 66:538–547.

Mukhopadhyay S, Fangueiro R (2009) Physical modification of natural fibers and thermoplastic films for composites - A review. J Thermoplast Compos Mater 22:135–162.

Nagalakshmaiah M, Afrin S, Malladi RP, Elkoun S, Robert M, Ansari MA, Svedberg A, Karim Z (2019) Biocomposites: Present trends and challenges for the future. Green Compos Automot Appl 197–215.

Ndlovu SS, Van Reenen AJ, Luyt AS (2013) LDPE-wood composites utilizing degraded LDPE as compatibilizer. Compos Part A Appl Sci Manuf 51:80–88.

Niang B, Ly EHB, Diallo AK, Schiavone N, Askanian H, Verney V, Badji AM, Diakite MK, Ndiaye D (2018) Study of the Thermal, Rheological, Morphological and Mechanical Properties of Biocomposites Based on Rod-Of Typha/HDPE Made up of Typha Stem and HDPE. Adv Mater Phys Chem 08:340–357.

Onuaguluchi O, Banthia N (2016) Plant-based natural fibre reinforced cement composites: A review. Cem Concr Compos 68:96–108.

Ordoudi S, Bakirtzi C, Tsimidou M (2018) The Potential of Tree Fruit Stone and Seed Wastes in Greece as Sources of Bioactive Ingredients. Recycling 3:1–19.

Painter P, Coleman M (2008) Processing. In: Essentials of Polymer Science and Engineering. Destech Publications, Inc., Lancaster, PA, pp 473–514.

Passaglia E, Coiai S, Augier S (2009) Control of macromolecular architecture during the reactive functionalization in the melt of olefin polymers. Prog Polym Sci 34:911–947.

Pelentir N, Block JM, Monteiro Fritz AR, Reginatto V, Amante ER (2011) Production and chemical characterization of peach (Prunus persica) kernel flour. J Food Process Eng 34:1253–1265.

Perinović S, Andričić B, Erceg M (2010) Thermal properties of poly(l-lactide)/olive stone flour composites. Thermochim Acta 510:97–102.

Peters DJ, Constabel CP (2002) Molecular analysis of herbivore-induced condensed tannin synthesis: Cloning and expression of dihydroflavonol reductase from trembling aspen (Populus tremuloides). Plant J 32:701–712.

Pickering KL, Efendy MGA, Le TM (2016) A review of recent developments in natural fibre composites and their mechanical performance. Compos Part A Appl Sci Manuf

83:98–112.

Pickering KL, Li Y, Farrell RL, Lay M (2007) Interfacial modification of hemp fiber reinforced composites using fungal and alkali treatment. J Biobased Mater Bioenergy 1:109–117.

Puglia D, Terenzi A, Barbosa SE, Kenny JM (2008) Polypropylene-natural fibre composites. Analysis of fibre structure modification during compounding and its influence on the final properties. Compos Interfaces 15:111–129.

Qian S, Igarashi T, Nitta KH (2011) Thermal degradation behavior of polypropylene in the melt state: Molecular weight distribution changes and chain scission mechanism. Polym Bull 67:1661–1670.

Rabaçal M, Fernandes U, Costa M (2013) Combustion and emission characteristics of a domestic boiler fired with pellets of pine, industrial wood wastes and peach stones. Renew Energy 51:220–226.

Rahma EH, El-Aal MHA (1988) Chemical characterization of peach kernel oil and protein: Functional properties, in vitro digestibility and amino acids profile of the flour. Food Chem 28:31–43.

Rana AK, Mandal A, Mitra BC, Jacobson R, Rowell R, Banerjee AN (1998) Short jute fiber-reinforced polypropylene composites: Effect of compatibilizer. J Appl Polym Sci 69:329–338.

Rolando Z, Bjornbom E (1999) Preparation of activated carbons from cherry stones , apricot stones and grape seeds for removal of metal ions from water. In: 2nd Olle Indstorm Symposium on renewable Energy-Bioenergy. Stockholm, Sweden, pp 46–50.

Rong MZ, Zhang MQ, Liu Y, Yang GC, Zeng HM (2001) The effect of fiber treatment on the mechanical properties of unidirectional sisal-reinforced epoxy composites. Compos Sci Technol 61:1437–1447.

Rosa SML, Santos EF, Ferreira CA, Nachtigalt SMB (2009) Studies on the properties of rice-husk-filled-PP composites - Effect of maleated PP. Mater Res 12:333–338.

Rowell RM et al, Sanadi A, Caulfield D, Jacobson R (1997) Utilization of natural fibers in plastic composites: Problems and opportunities lignocellulosic-plastics composites. Lignocellul Compos 15:23–51.

Roy Choudhury AK (2017) Various ecofriendly finishes. In: Principles of Textile Finishing. Woodhead Publishing, pp 467–525.

Rzayev ZMO (2011) Graft copolymers of maleic anhydride and its isostructural analogues: High performance engineering materials. Int Rev Chem Eng 3:153–215.

Sagar NA, Pareek S, Sharma S, Yahia EM, Lobo MG (2018) Fruit and vegetable waste: Bioactive compounds, their extraction, and possible utilization. Compr Rev Food Sci Food Saf 17:512–531.

Santos EF, Mauler RS, Nachtigall SMB (2009) Effectiveness of maleated- and silanized-PP for coir fiber-filled composites. J Reinf Plast Compos 28:2119–2129.

Selke S, Culter J (2016) Polymer Structure and Properties. In: Hamilton C (ed) Plastics Packaging Properties, Processing, Applications, and Regulations, 3rd edn. Hanser Publications, Cincinnati, Ohio, pp 23–100.

Shahbandeh M (2019) U.S. per capita consumption of fresh peaches and nectarines 2000-2018. In: Statista. https://www.statista.com/statistics/257229/per-capita-consumption-of-fresh-peaches-and-nectarines-in-the-us/#statisticContainer. Accessed 2 Jun 2020.

Shakeri AR, Hashemi SA (2004) Effect of coupling agents on mechanical properties HDPE/wheat straw composites. Polym Polym Compos 12:449–452.

Sharma S, Verma D (2016) Rice Husk Reinforcement in Polymer Composites. In: Sharma S, Verma D, Jain S, Chandra Gope P (eds) Green Approaches to Biocomposite Materials Science and Engineering. IGI Global, Hershey, PA, pp 165–191.

Shrivastava A (2018) Introduction to Plastics Engineering. In: Ebnesajjad S (ed) Introduction to Plastics Engineering, 1st edn. William Andrew Publishing, pp 1–16.

Singh T, Gangil B, Patnaik A, Biswas D, Fekete G (2019) Agriculture waste reinforced corn starch-based biocomposites: Effect of rice husk/walnut shell on physicomechanical, biodegradable and thermal properties. Mater Res Express 6:1–10.

Sinha E, Panigrahi S (2009) Effect of plasma treatment on structure, wettability of jute fiber and flexural strength of its composite. J Compos Mater 43:1791–1802.

Soroudi A, Jakubowicz I (2013) Recycling of bioplastics, their blends and biocomposites: A review. Eur Polym J 49:2839–2858.

Sri Aprilia NA, Abdul Khalil HPS, Bhat AH, Dungani R, Hossain MS (2014) Exploring material properties of vinyl ester biocomposites filled carbonized Jatropha seed shell. BioResources 9:4888–4898.

Sultana N, Khan TH (2013) Water absorption and diffusion characteristics of nanohydroxyapatite (nHA) and poly(hydroxybutyrate-co-hydroxyvalerate-) based composite tissue engineering scaffolds and nonporous thin films. J Nanomater 2013:1–8.

Tanaka T, Ito H (2013) Manufacturing and processing methods of biocomposites. In:

Thomas S, Joseph K, Malholtra S, et al. (eds) Polymer Composites, Biocomposites. Wiley, pp 179–211.

Tawakkal ISMA, Talib RA, Abdan K, Ling CN (2012) Mechanical and physical properties of kenaf-derived cellulose (KDC)-filled polylactic acid (PLA) composites. BioResources 7:1643–1655.

Thomas S, Joseph K, Molhotra S, Goda K, Sreekala M (2013) Manufacturing and Processing Methods of Biocomposites Vol. 3. In: Thomas S, Joseph K, Molhotra S, et al. (eds) Polymer Composites: Biocomposites. Wiley, Hoboken, NJ, pp 179–209.

Torrens Zaragozá F (2015) Classification of fruits proximate and mineral content: Principal component, cluster, meta-analyses. Nereis Rev Iberoam Interdiscip métodos, Model y simulación 1:39–50.

Torres-León C, Ramírez-Guzman N, Londoño-Hernandez L, Martinez-Medina GA, Díaz-Herrera R, Navarro-Macias V, Alvarez-Pérez OB, Picazo B, Villarreal-Vázquez M, Ascacio-Valdes J, Aguilar CN (2018) Food waste and byproducts: An opportunity to minimize malnutrition and hunger in developing countries. Front Sustain Food Syst 2:1–17.

Tragoonwichian S, Yanumet N, Ishida H (2007) Effect of fiber surface modification on the mechanical properties of sisal fiber-reinforced benzoxazine/epoxy composites based on aliphatic diamine benzoxazine. J Appl Polym Sci 106:2925–2935.

Treece MA, Oberhauser JP (2007) Processing of polypropylene-clay nanocomposites: Single-screw extrusion with in-line supercritical carbon dioxide feed versus twin-screw extrusion. J Appl Polym Sci 103:884–892.

USDA NASS (2020) Noncitrus Fruits and Nuts 2019 Summary. Washington, DC.

Väisänen T, Batello P, Lappalainen R, Tomppo L (2018) Modification of hemp fibers (Cannabis Sativa L.) for composite applications. Ind Crops Prod 111:422–429.

Valadez-Gonzalez A, Cervantes-Uc JM, Olayo R, Herrera-Franco PJ (1999) Effect of fiber surface treatment on the fiber–matrix bond strength of natural fiber reinforced composites. Compos Part B Eng 30:309–320.

Van de Weyenberg I, Ivens J, De Coster A, Kino B, Baetens E, Verpoest I (2003) Influence of processing and chemical treatment of flax fibres on their composites. Compos Sci Technol 63:1241–1246.

Van Soest PJ, Robertson JB, Lewis BA (1991) Methods for Dietary Fiber, Neutral Detergent Fiber, and Nonstarch Polysaccharides in Relation to Animal Nutrition. J Dairy Sci 74:3583–3597.

Velde K Van De, Kiekens P (2003) Effect of flax /PP panel process parameters on resulting composite properties. J Thermoplast Compos Mater 16:413–431.

Venkatachalam N, Navaneethakrishnan P, Rajsekar R, Shankar S (2016) Effect of pretreatment methods on properties of natural fiber composites: A review. Polym Polym Compos 24:555–566.

Vilaplana F, Strömberg E, Karlsson S (2010) Environmental and resource aspects of sustainable biocomposites. Polym Degrad Stab 95:2147–2161.

Viorica-Mirela G, Socaciu C, Jianu I, Florica R, Florinela F (2006) Identification and quantitative evaluation of amygdalin from agricot, plum and peach oils and kernels. BullUSAMV-CN 2006:246–253.

Wadhwa M, Bakshi M, Makkar H (2016) Wastes to worth: value added products from fruit and vegetable wastes. CAB Rev Perspect Agric Vet Sci Nutr Nat Resour 10:1–25.

Wang B, Panigrahi S, Tabil L, Crerar W (2007) Pre-treatment of flax fibers for use in rotationally molded biocomposites. J Reinf Plast Compos 26:447–463.

Wang X, Jia Y, Liu Z, Miao J (2018) Influence of the Lignin Content on the Properties of Poly(Lactic Acid)/lignin-Containing Cellulose Nanofibrils Composite Films. Polymers (Basel) 10:1013.

Wu F, Liu C, Sun W, Zhang L (2018) Mechanical properties of bio-based concrete containing blended peach shell and apricot shell waste. Mater Technol 52:645–651.

Yang HS, Kim HJ, Park HJ, Lee BJ, Hwang TS (2006) Water absorption behavior and mechanical properties of lignocellulosic filler-polyolefin bio-composites. Compos Struct 72:429–437.

Yang HS, Wolcott MP, Kim HS, Kim HJ (2005) Thermal properties of lignocellulosic filler-thermoplastic polymer bio-composites. J Therm Anal Calorim 82:157–160.

Yang J, Ching YC, Chuah CH (2019) Applications of lignocellulosic fibers and lignin in bioplastics: A review. Polymers (Basel) 11:1–26.

Yang Y, Boom R, Irion B, van Heerden D-J, Kuiper P, de Wit H (2012) Recycling of composite materials. Chem Eng Process Process Intensif 51:53–68.

Zhang L, Lv S, Sun C, Wan L, Tan H, Zhang Y (2017) Effect of MAH-g-PLA on the Properties of Wood Fiber/Polylactic Acid Composites. Polymers (Basel) 9:1–14.

Zhang R, Zhu Y, Zhang J, Jiang W, Yin J (2005) Effect of the initial maleic anhydride content on the grafting of maleic anhydride onto isotactic polypropylene. J Polym Sci Part A Polym Chem 43:5529–5534.

Zhu ZH, Mo BH, Hao MY (2019) Study of contents ratio of cellulose, hemicellulose and lignin on the mechanical properties of sisal fibers reinforced polylactic acid (PLA) composites. IOP Conf Ser Mater Sci Eng 544:.

Zykova AK, Pantyukhov P V., Kolesnikova NN, Popov AA, Olkhov AA (2015) Influence of particle size on water absorption capacity and mechanical properties of polyethylene-wood flour composites. AIP Conf Proc 1683:1–4.